II

63 Mountain Green Circle,
Candlewood, Quail Meadows Estate,
Windsor Mill, MD 21244-2602

October 1, 2001

Commission of Patents and Trademarks,
Washington, DC 20231

Subject: Disclosure Document Program

Invention: Parametric Ultrawide Band Sounder (PUBS™)
Non-Intrusive Remote Sensor System

Inventor: Frank L. Rees

Dear Sir or Mesdame:

The undersigned, being an inventor of a Parametric Ultrawide Band Sounder (PUBS™) Non-Intrusive Remote Sensor System utilizing a Gauss-Rees Primary Wave to produce a quasi-Ricker Secondary Wavelet – with properties consistent with inverted Mexican hat mother wavelet analysis – through far-field interaction using a Self-Demodulating/NonLinear Sonic (SD/NLS) system, request that the enclosed papers (32 pages) be accepted under the Disclosure Document Program, and that they be preserved for a period of two years. In addition, the intent is to file for the PUBS™ trademark, which trademark, from hereon, will be marked accordingly. A cheque for the amount of $ 10.00, payable to "Commissioner of Patents and Trademarks, Washington, DC 20231" is enclosed to cover the fee.

I have also enclosed a duplicate of this cover letter and the disclosure document, together with a stamped-addressed envelope for certification and return to me.

Very respectfully,

X Frank L. Rees

Frank L. Rees, Inventor.

Tel: (410) 944-6629 (Voice)/4642 (Fax)

PARAMETRIC ULTRAWIDE BAND SOUNDER (PUBS™)

By Combining:

- A Primary Waveform composed of a Gauss-Rees envelope modulation function for gating a Continuous Wave (CW) carrier operating at a frequency capable of forming several carrier cycles inside of the Gauss-Rees envelope

- Self-Demodulating/NonLinear Sonic (SD/NLS) interaction in either an air or a liquid fluid medium, wherein, such an interaction is designed to create an approximately 5:1 frequency "down-shift" while forming a (100 % band-width/touching base-band/zero mean) quasi-Ricker, otherwise known as an inverted Mexican-hat, Secondary Wavelet for penetration of even very thick enclosure walls in order to provide non-intrusive, remote sensing *via* "impulse" excitation of the backward, off-axis or forward (i.e., trans-ensonification) scattering from various molecular compounds as the constituents of certain (possibly illicit) materials that otherwise would be obscured: say by being:- a) inside of the walls of a container (e.g, a container cargo holder or storage container or room or carrying case, *etc.*); or b) explosives enclosed in the casings of certain land-mines buried in sandy terrain or sea-mines buried in the sea-bottom mud; or c) hydrocarbon deposits buried in relatively deep strata of the earth that are either accessible through petroleum drilling from the earth's surface or from oil-rig platforms mounted in deep water areas of the Continental Shelf; or d) hidden in a vehicle (e.g., an automobile or truck or speed boat or commercial or general aviation aircraft, *etc.*); or e) hidden in any other enclosure that is penetrable by "impulse" acoustic imaging/spectroscopy as a means to reveal and identify concealed materials

- A narrowly directed, very low side-lobe beam formed from a small sound projector operated at the Primary Waveform frequency that – through SD/NLS interaction in the particular fluid in which such a container or vehicle is immersed, buried or operated – somewhat enhances these desirable beam-ensonification characteristics when "down-shifted" to a touching base-band region of frequency in the process of forming a Secondary Wavelet

- A receiver array of either ultrawide-band microphones or hydrophones for, respectively, collecting in-air or underwater "target" scattered signals to be amplified through a low-noise, sensitive ultrawide-band "impulse" response receiver optimized to signal-process Mexican hat or inverted Mexican hat Secondary Wavelets

- A spectroscopic analyzer for identifying the molecular structure of the obscured material through the appearance of spectral components induced by nonlinear-acoustic interaction or inelastic-acoustic scattering within the material

To Provide:

- A non-intrusive way of remote sensing both the morphology and material content of concealed materials

I Have Invented:

- A Parametric Ultrawide Band Sounder (PUBS™) system which will provide better enclosure penetration than Ultra Wide Band (UWB) radar while having equivalent resolving power to examine the constituted material morphology through imaging and, in addition, provide material properties through spectroscopic examination of nonlinear-acoustic properties or inelastic-acoustic scattering

Attested by Inventor:

Frank L. Rees

Frank L. Rees
Inventor
October 1, 2001

Witnessed and Understood by:

Witnessed and Understood by:

Name: _____ Date: 10/18/01 Name: _____ Date: 10/18/01

Caveat to the Invention:

Parametric Ultrawide Band Sounder (PUBS™) system represents a generic technique and associated technology submission made under the U.S Patent and Trademarks Patent Disclosure Program. As indicated in the introductory description preceding the signature portion, it covers a wide range of potential applications. Some of these applications may already be committed to certain device manufacturers *via* previous business or non-disclosure agreements. Examples of this are:- i) the Parametric Ultrawide-band Tomography (PUT™) scan medical-electronics application; ii) the Parametric, Repeatable-Impulse Seismic Exploration (PRISE™) source intended for both land-based and marine-based hydrocarbon exploration applications; and, also, iii) the Parametric Airborne Dipping Sonar-Hosting Ultrawide Band Sensing (PADS-HUBS™) subsystem intended for providing the PADS system with a PUBS™ waveform mode-of-operation for "impulse" waveform enhanced Anti-Submarine Warfare (ASW) and Anti-Surface Unit Warfare (ASUW) sonar and (e.g., buried) Mine Hunting activity. In other cases, preliminary interest in obtaining the rights to certain other applications has been expressed. One recent example is the Parametric Radiator for Aviation Interrogation through Sound Evaluation (PRAISE™) sensor application for, in particular, determining that general aviation aircraft are not carrying Chemical and Biologic Weapons (C&BW), explosives, small nuclear bomb devices or a Flux Compression Generator (FCG) conventional-bomb type of Electro-Magnetic Pulse (EMP) generator, *etc.* No doubt there will be other applications for the PUBS™ technology, many of which might parallel but vastly improve upon or complement the use of Ultra Wide Band (UWB) radar.

Indeed, the range of applications for the PUBS™ technology is so broad, and Gauss-Rees Primary Waveform quite ***innovative***. Wherein, the obscurity of this ***unique*** derivation is specific to unsaturated Self-Demodulating/Non-Linear Sonic (SD/NLS) **far-field** interaction. This is opposed to the more obvious case for **near-field** interaction (which has a very restricted range of applications in the ultrasonic Secondary Wavelet frequency region demanded by Primary Waveform projector **near-field** absorption limiting considerations). For this reason, the generic PUBS™ technology is claimed to be the ***exclusive*** Intellectual Property of the undersigned as its inventor. As with the U.S. Supreme Court resolution of ownership in favor of the individual that claimed to have ***invented*** the UWB radar technique and associated technology, in opposition to the Lawrence-Livermore Laboratories that pursued it for more narrow applications, this legal precedence bears direct relationship to the PUBS™ technique and associated technology.

In pursuing the indicated and other potential applications of PUBS™, the intent is to negotiate and fully ratify business agreements with a prospective assignee of any ensuing application patent that will be ***unequivocally*** issued in the sole name of the undersigned as its inventor. The business agreement will identify compensation terms. However, in doing so, it will stipulate that the assignee (as an individual or corporate entity) will bear all costs of obtaining the desired patent coverage and provide the total wherewithal to "reduce-to-practice" the device or product covered by such an application patent whose antecedent is the PUBS™ system. Furthermore, U.S. Trademark coverage also will be sought and adhered to through the continual use of the trademark sign.

Theoretical Precepts of the Invention:

As a facet of nonlinear acoustics in various solid, liquid or gas media, NonLinear Sonar (NLS) – wherein, the word Sonar, that usually implies an underwater sound equivalent of radar, is altered to Sonic – systems, sometimes, are synonymously referred to as a Parametric Sonar or Parametric Sonic or Parametric Sounder system. This is because of the parametric nature of the mechanism that alters both the local existing bulk modulus, $\kappa(p(\mathbf{x}, t))$, and density, $\rho(p(\mathbf{x}, t)$, as a parametric function of the local space-time – i.e., a possible three-dimensional spatial position vector, $\mathbf{x}$, and a time, t – varying pressure wave, $p(\mathbf{x}, t)$, in the medium through which a nonlinear-acoustic wave travels. As a consequence, the corresponding "large acoustic signal" nonlinear-acoustic traveling wave pressure ***fluctuation***, $p'(\mathbf{x}, t) = p(\mathbf{x}, t) - p_0$, progresses at a phase wave speed given by a space-time varying quantity $c(p(\mathbf{x}, t)) = [\kappa(p(\mathbf{x}, t))/\rho(p(\mathbf{x}, t))]^{1/2}$. In these various expressions, the superscript ′ is used to indicate the ***fluctuations*** or ***variations*** from their ambient values that are indicated by the subscript $_0$ placed on each of the independent and dependent variables, $\kappa(p(\mathbf{x}, t)) = \kappa'(p(\mathbf{x}, t)) + \kappa_0$, $\rho(p(\mathbf{x}, t)) = \rho'(p(\mathbf{x}, t)) + \rho_0$, $p(\mathbf{x}, t) = p'(\mathbf{x}, t) + p_0$ and $c(p(\mathbf{x}, t)) = c'(p(\mathbf{x}, t)) + c_0$, for the ambient medium values of bulk modulus, $\kappa_0 = \kappa(p_0)$, and density, $\rho_0 = \rho(p_0)$, as a function of the medium ambient (mean) pressure, p_0, and the "small acoustic signal" ambient acoustic phase wave speed $c_0 = [\kappa_0/\rho_0]^{1/2}$.

These formulations are provided to facilitate discussion about the nature of nonlinear-acoustic traveling waves. At "large acoustic signal" levels the speed-of-sound varies during the progression of a nonlinear acoustic wave. (This is opposed to the so called "small acoustic signal" levels used to describe conventional underwater sonar or in-air sonic wave propagation; that ignores the effects of compression of the medium on the bulk modulus and density values as an acoustic wave progresses through the medium.) In fact, as a large positive pressure "swing" of a propagating wave locally increases the pressure of the medium above its ambient value, the wave locally travels faster than the "small-signal" speed-of-sound, c_0. Conversely, for a large negative pressure "swing", the wave locally travels below c_0. The consequence of this is that, under these conditions, the "peak" of a propagating nonlinear-acoustic wave "out-runs" its associated "trough." In doing this, a sinusoidal (mono-frequency, f_0) traveling wave would become "saw-toothed" in its shape; thereby, being composed of a family of harmonics ($f_n = n f_0$, $n = 1,2,\ldots\ldots$) of the fundamental frequency, f_0, of the original mono-frequency wave.

Components of this harmonic family inter-modulate with each other to form new components given by $f_{m,n} = f_m \pm f_n = (m \pm n) f_0$. Generally speaking, the inter-modulation components associated with the + sign do not propagate very well because of the increase of acoustic-energy absorption that attends an increasing frequency of a propagating acoustic wave. This also generally holds for the non-inter-modulated harmonics having values of n greater than unity. In turn, the negative sign generally favors lower-frequency propagation through the medium. In fact, this form of inter-modulation due to nonlinear-acoustic interaction gives rise to Secondary Wave components that are "down-shifted" in frequency from the original Primary Wave frequency to a frequency location "touching base band" by a process called Self-

Demodulation (SD) interaction. Underwater NonLinear Sonar systems or in-air NonLinear Sonic systems that utilize this nonlinear-acoustic interaction mechanism are called SD/NLS systems. Respectively, they also are called self-demodulating parametric sonar or self-demodulating parametric sonic systems.

Basic nonlinear-acoustic interaction phenomena such as "saturation" and the corresponding "critical-pressure" levels associated with the onset of underwater "weak shock" or in-air "shock" are best described and quantified in terms of mono-frequency waves. However, the mid-to-late 20 th century emergence of underwater NLS (or, as sometimes known, parametric sonar) from knowledge of nonlinear acoustics dating back to the 19 th century arose from the consideration of something called Dual-Wave (DW) interaction. Underwater NonLinear Sonar systems utilizing this mechanism are known as DW/NLS systems; whereas, analogous NonLinear Sonic systems that arose somewhat later are also known as DW/NLS systems where the S, respectively, designates a Sonar or Sonic system. Of course, replacing a mono-frequency carrier wave with a dual-frequency pair of carrier waves requires twice as much acoustic power to reach a particular level.

As the name implies the DW/NLS system involves the projection of two acoustic beams that overlap each other in the form of a pair of coterminous traveling nonlinear-acoustic waves. The dual carrier waves each have any individual form of amplitude modulation and/or phase modulation centered at two respectively different frequencies, f_1 and f_2. Unlike the SD/NLS system, any modulation spectrum on each of the carriers of the DW/NLS system Primary Waves has to have a bandwidth ratio small enough that their individual (possibly different) spectra do not overlap each other. Whereas, the only constraint on the SD/NLS system Primary Wave modulation bandwidth is that it does not overlap the Secondary Wave base-band SD spectrum.

In the DW/NLS system case, the inter-modulation products generated when these two carrier-borne nonlinear-acoustic waves interact are given by $f_{m,n}^{\pm} = m f_2 \pm n f_1$. The possible principal Secondary Waves generated from the Dual Primary Waves are the difference frequency $f_{1,1}^{-} = f_2 - f_1$ and the sum frequency $f_{1,1}^{+} = f_2 + f_1$. Wherein, it is to be recognized that the difference-frequency Secondary Wave, generally, propagates over longer distances than its sum-frequency counterpart. This is because of the previously mentioned excess acoustic absorption losses attending the sum-frequency Secondary Wave relative to its difference-frequency counterpart.

(It is to be noted that, when $f_1 = f_2 = f_0$, after adjustment of the combined amplitude of the dual waves – that are assumed to be coherent with each other – the DW/NLS and SD/NLS systems, in concept, behave identically. In other words, under the above assumption, a SD/NLS system may be treated as a subset of a DW/NLS system. Of course, this is only conceptually so because the inter-modulation components and the projector power-amplifier/transducer-array hardware of any DW/NLS system and any SD/NLS system, obviously, would have a quite different components and subsystem configurations, as would an associated receiver.)

Returning to the mono-frequency carrier wave, the so quantified "saturation" criterion punctuates the difference between "unsaturated" and "saturated" nonlinear-acoustic wave performance for both the SD/NLS and DW/NLS systems. There is a change in "conversion efficiency" depending upon whether or not the peak-amplitude "swing" of a "large-signal" nonlinear-acoustic wave remains below the "critical shock" level. The form of "shock" referred to in the term "critical shock" level is considered to be "weak shock" in the underwater case or the type of "shock" known to occur in air. Either way, a "shock front" occurs within the steep "trailing-edge return" portion of the "saw-tooth" carrier waveform that is generated by the previously mentioned nonlinearly induced peak/trough dispersion in the speed-of-sound respectively in water or in air.

The "conversion efficiency" is defined as the power ratio (usually converted to decibels) of the Secondary Wave acoustic power to Primary Wave acoustic power; wherein, the Primary Wave (effective) acoustic power also suffers some depletion due to power lost in creating harmonics. In the "unsaturated" nonlinear-acoustic interaction case, the "conversion efficiency" increases by 10 dB for every 10 dB increase in the Primary Wave (effective) acoustic power; thereby resulting in a 20 dB increase in the Secondary Wave acoustic power until the Primary Wave amplitude approaches the "critical-shock" level. However, over a region of Primary-Wave amplitude from the "critical-shock" level to about 10 dB or so above it, the "conversion efficiency" starts to "flatten-out" – of course, with a "fairing-in" region occurring around the "critical-shock" level – and remains substantially constant as the Primary Wave (effective) acoustic power continues to climb by another 10 dB; thereby resulting in a 10 dB increase in the Secondary Wave acoustic power. Beyond this region of the "saturated" range, a catastrophic demise of "conversion efficiency" occurs because the steepness of the "shock front" region is eroded by viscous losses and no further increase in Secondary Wave acoustic power results from further increasing the Primary Wave (effective) acoustic power. This is rapidly depleted by viscous losses that heat the propagation medium. (In the case of water, this action also causes cavitation that was shown by Soviet researches to have a beneficial action in forestalling this catastrophic demise.)

Another thing that affects "conversion efficiency" is the "down-shift" ratio. It does so in a different fashion depending upon whether the nonlinear-acoustic interaction is "unsaturated" or "saturated." Regardless, a good "rule-of-thumb" is to keep the "down-shift" ratio below 10:1. In fact, most usable SD/NLS or DW/NLS system designs attempt to stay closer a 5:1 "down-shift" ratio. Of course, all system-design "trade-offs" should be performed or, as a close-to-final system design, checked using a high-fidelity nonlinear-acoustic interaction model.

At this juncture, near-field interaction or far-field interaction of nonlinear-acoustic waves needs to be described. There is a transition range at which the near-field behavior of the Primary Wave projector array gives way to a far-field behavior. This so-called "Rayleigh transition range", for a square or circular aperture, is given by the aperture area, S, divided by the wavelength, λ_0, of the Primary Wave acoustic carrier for a SD/NLS system; which, for convenience, is taken at the geometric-mean frequency when DW/NLS system twin frequencies are involved. When rectangular or elliptical apertures

are involved – as they would be if different beam-widths were desired in the azimuth and the elevation directions – the "Rayleigh transition range varies respectively with the eccentrically different orthogonal dimensions of this type of aperture.

Near-field interaction results from the case where absorption (plus harmonic depletion) limits the region where either SD or DW inter-modulation efficiently occurs to being in the near field of the acoustic radiating projector. It must be remembered that, once the residual Primary Wave acoustic amplitude drops too far below the "critical-shock" level as a result of acoustic-absorption and harmonic-depletion losses, the "conversion efficiency" may have diminished below where it is significant. In that acoustic absorption causes an exponential decay of the Primary Wave traveling wave field as it progresses outward through the near-field region, the famous Rutherford neutron scattering pattern of nuclear physics arises. This Rutherford Secondary-Wave acoustic beam pattern has no side lobes; and, although it broadens somewhat in the off-main-lobe direction, when harmonic-depletion losses become significant, it still does not exhibit side lobes. There is a major drawback of employing a near-field interacting SD/NLS or DW/NLS system. It is that, except for extending the near-field distance with enormously over-sized apertures, such a condition only is realistically attainable at quite high acoustic frequencies; wherein, range coverage will be severely limited by acoustic absorption of the Secondary Wave.

Far-field interaction is only significant when only a minor amount of acoustic-absorption and/or harmonic depletion is accomplished within the near field. This usually is the case when lower Primary-Wave frequencies and a 5:1 "down-shift" ratio are employed in to provide a SD/NLS or DW/NLS system Secondary-Wave source that is designed to achieve relatively long propagation ranges. Usually, sound sources at such low Secondary-Wave frequencies will penetrate containers and, thereby, sustain both nonlinear-acoustic interaction and inelastic scattering within enclosed materials. In this case, far-field nonlinear interaction continues even in the face of acoustic-propagation "spreading losses" because the wave-front area over which this nonlinear interaction occurs is increasing in a like manner. However, viscous losses and harmonic depletion eventually cause "old age" and no further nonlinear conversion results to further "pump" and, thereby, continue to amplify the Secondary Wave.

Recalling that a SD/NLS system is conceptually a subset of a DW/NLS system, the far-field interaction beam formation mechanism will be described for the latter case as a generality of the former case. In the far field, the pattern resulting from two overlapping DW/NLS system Primary Wave beams supporting the coterminous traveling dual waves drops-off in amplitude according to the product of the twin beams. (Obviously, this "product" beam pattern of the DW/NLS system becomes a "square-law" beam pattern for the SD/NLS.) Consequently, by virtue of the "conversion-efficiency" behavior of an "unsaturated" far field interacting DW/NLS system, the Secondary Wave beam pattern also drops-off in accord with the Primary Wave "product" pattern. (It also is to be noted that this becomes a "square-law" beam pattern in the SD/NLS system case.) As a consequence of the projected near-field interaction being taken over by a dominant far-field interaction, a DW/NLS system has a composite beam pattern. It has been shown

theoretically that this is given by the spatial convolution of a Rutherford beam pattern with a "product" (or, in the case of a SD/NLS system, a "square-law") beam pattern.

Usually, the main lobe of most types of beam patterns fits reasonable closely to a Gaussian-shaped beam pattern; as also does the main lobe of a Rutherford beam pattern. Therefore, a useful approximation to the 3-dB beam-width of the composite beam pattern arising from either near-field or far-field "unsaturated" interaction for a DW/NLS system is given by the formula $\theta^2 = \{1/[(1/\theta_1)^2 + (1/\theta_2)^2]\} + \theta_R^2$; where the composite beam-width is obtained by extracting the square-root of each side of this equation. Likewise, the same formula applies if ϕ_1 and ϕ_2 the elevation pattern beam-width respectively of the dual waves along with ϕ_R as the Rutherford-pattern beam-widths, respectively, are substituted for their θ_1, θ_2 and θ_R azimuth pattern beam-width counterparts.

It is to be recognized that the composite pattern beam width of a far-field interacting SD/NLS system may be determined by invoking that the common "square-law" pattern 3-dB beam-width θ_0 be given by setting $\theta_0 = \theta_1 = \theta_2$ and, likewise, $\phi_0 = \phi_1 = \phi_2$. When the far-field interacting DW/NLS system "product" (or the SD/NLS system "square-law") beam width becomes increasingly narrower than the Rutherford pattern beam-width the above formulations indicate that (θ, ϕ) tend towards the Rutherford pattern beam-widths (θ_R, ϕ_R). This happens, conceptually, when the choice of system parameters is altered towards making either one into a near-field interacting system. In other words, in the far-field interaction limit, the spatial convolution regards the Rutherford beam pattern as delta-Dirac function; whereas, in the near-field interaction limit, it is the "product" or the "square-law" beam pattern that is so regarded.

In terms of a pair of traveling Primary-Wave ***temporal*** pressure waveforms of a DW/NLS system, the analytic-signal (i.e., complex) relationship for the Secondary Wave – or, in the special case of certain applications of a SD/NLS system, a temporal-wavelet – from near-field interaction may be derived by applying ***spatial*** integrals over a form:-

$$\varphi_S(\mathbf{x}, t\,|\theta, \phi) \approx -\{[D_R(\theta, \phi)\,\beta\, S\, p_1\, p_2]/8\pi\rho_0 c_0^4\, \alpha_T r\}\, \exp(-\alpha_S r) \times \{\partial^2\, [\varphi_1(\mathbf{x}, t')\varphi_2^*(\mathbf{x}, t')]/\partial t'^2\}.$$

Using the asymptotic form of one of the same set of integrals from which the near-field interacting DW/NLS system case was derived, the far-field interaction counterpart is:-

$$\varphi_S(\mathbf{x}, t\,|\theta, \phi) \sim -\{[D_1(\theta, \phi)\, D_2^*(\theta, \phi)\,\beta\, r_0^2\, p_1\, p_2]/2\rho_0 c_0^3\, r\}\, [\ln(\pi^2 f_S/\alpha_T c_0)]\, \exp(-\alpha_S r) \times \{\partial[\varphi_1(\mathbf{x}, t')\varphi_1^*(\mathbf{x}, t')]/\partial(\mathbf{x}, t')\}.$$

Herein, the retarded-wave clock operates at a time given by $t' = t\,[1 - (r/c_0)]$; where c_0 is the "small-signal" speed-of-sound in the medium. The analytic forms of the dual ***space-time*** pressure waves are given by $\varphi(\mathbf{x}, t')$ and $\varphi(\mathbf{x}, t')$; where * represents that a complex-conjugation operation is performed. The composite acoustic absorption coefficient is $\alpha_T = \alpha_1 + \alpha_2 - \alpha_S$; where α_1, α_2 and α_S, respectively, are the acoustic absorption at each of the dual Primary-Wave and Secondary-Wave frequencies; wherein, in the DW/NLS

system case, the latter frequency is called the difference frequency. The quantity S is the Primary-Wave projector area and the Source Level (SL) is referred to a particular value of the radial-range, r, called the reference distance, r_0; wherein, r_0 usually is taken at one meter from the face of the Primary-Wave projector. The peak-pressure levels associated with the SLs for the dual waves of a DW/NLS system are p_1 and p_2. In addition, the azimuth angle is θ and the elevation angle is ϕ; where $D_1(\theta, \phi)$, $D_2(\theta, \phi)$ and $D_R(\theta, \phi)$ are the complex-amplitude beam patterns, respectively, of the twin Primary-Wave (far-field interaction) beams # 1 and # 2 and the (near-field interaction) Rutherford beam. It also is to be noted that the natural logarithm term, $\ln(\pi^2 f_S/\alpha_T c_0)$, arises from one of the original multiple integrals (in the ***spatial*** integral set). It acts as a weighting coefficient applied to a delta-Dirac function that is used to approximate a very narrow Rutheford beam pattern that appears in the far-field interaction beam-pattern convolution integral.

Finally, β is a coefficient representing the nonlinear properties of the material in which nonlinear-interaction occurs. In fact, in progressing along the whole propagation path, nonlinear interaction may well occur sequentially while passing through several cascaded media. For example, this also may entail nonlinear interaction occurring sequentially in passing through the main propagation medium, then through the wall of an enclosure and into the concealed material being subjected to non-intrusive, remote sensing. Of course, in a seismic-exploration application, ultimately, this will entail passing through stratified layers of the Earth's crust to reach concealed hydrocarbons.

Motivation for the Invention:

Clearly, the most important factor from a material properties viewpoint is $\beta = 1 + (B/2A)$; where A and B/2, respectively, are the coefficients of the s and s^2 terms in a power series expansion of the excess pressure, $p' = p - p_0$, in terms of the condensation $s = (\rho - \rho_0)/\rho_0$. In addition, the A-coefficient is the $p = p_0$ value of the bulk modulus (namely, the ambient bulk modulus, κ_0), and ρ_0 is the ambient density of the material in which nonlinear-acoustic interaction is taking place. It has been shown that A and B are quite unique between materials and control any form of nonlinear-acoustic hysteresis that relates to the generation of sub-harmonics as well as the usual harmonic sets of spectral lines. Hysteresis arises from additional terms in an expansion of the pressure dependency of the speed-of-sound in a medium, namely $c(p) = c_0 + c_0 [1 + (B/sA)] [p'/\rho_0 c_0^2)] + etc.$

In a similar way, Nuclear Magnetic Resonance (NMR) spectroscopy – which is a process fundamental to Magnetic Resonance Imaging (MRI) – evolved from the exploitation of nonlinear magnetic-spin interactions. These nonlinear interactions are revealed under a strong DC magnetic alignment through the application of Radio Frequency (RF) Electro-Magnetic (EM) field perturbations and by interrogating the subsequent energy-state relaxations. The favored way of doing this perturbation involves "impulse" excitation with RF fields, which suggests that a SD/NLS system producing an ultrawide-band sonic "impulse" excitation has the potential to yield analogous signatures.

Additionally, French and, previously, Soviet researchers have explored nonlinear-acoustic analogies of nonlinear-optics energy state interchanges and inelastic scattering.

French researchers at the Université d' Grenoble have uncovered ways of producing Sound Amplification by Stimulated Emission of Radiation (SASER) analogs of optical lasers. Among other analogies, the Soviet researchers at the Institute of General Physics, Academy of Sciences of the USSR also had demonstrated acoustic versions of a method for producing optical Stimulated Raman Scattering (SRS). Both these analogies, and the NMR analogy, have motivated the spectroscopic-analysis aspect of the invention of the generic **P**arametric **U**ltrawide **B**and Sounding (PUBS™ system technique and associated technology applications.

In the earlier days, it was high-resolution acoustic imaging that motivated the invention of the nonlinear acoustically generated ultrawide band "impulse" wavelet. It was observed that, generally speaking, marine seismic exploration sources rely upon the formation of a "bubble pulse" for the purpose of generating their relatively high-energy wavelet source for penetrating the stratified layers that reside beneath the sea floor. The amount of potential energy transferred into a "cavitation bubble" created by using, say, explosive charges, a "boomer", an air gun, multi-tip "sparker", *etc.*, is measured by an Energy Ratio (ER) that is quite small. In turn, when combined with the acoustic-radiation efficiency of such "cavitation bubbles" used as the mechanism for emitting underwater sound – that, ultimately, couples into seismic waves propagated in strata located below the sea floor – the overall efficiency is comparable to or worse than conversion efficiency of a SD/NLS system.

In addition to this important feature of SD/NLS system techniques for marine seismic-exploration technology, the ability to focus acoustic-source energy onto a desired region on the sea floor located directly under a seismic "streamer" also became obviously appealing. This was because the other types of marine seismic sources did not possess this desirable capability due to the relatively small (practically sized) source-to-acoustic wavelength ratio associated with the low frequencies typically employed for marine seismic exploration. Lack of transmission directionality causes undesirable "ghosting" and "peg-leg" artifacts as encountered in "stacking" multi-channel "streamer" data.

Another favorable aspect of using a SD/NLS system for marine seismic exploration is the ability to produce a highly repeatable wavelet having a desirable shape. One such wavelet shape known to land seismologists is called a Ricker wavelet; which is represented by plus/minus three-quarters-of-a-cycle of an inverted cosine wave (namely, a total of one-and-one-half cycles). This wavelet closely matches the "impulse" response of the Earth's crust. However, underwater wavelets have to have a zero temporal mean in order to meet natures requirement that the mean hydrostatic pressure be restored after the passage of such a wavelet without incurring secondary "ringing" pulses. For this reason, a quasi-Ricker wavelet having this zero-mean property is preferred. This quasi-Ricker wavelet is identical to an inverted Mexican-hat mother wavelet oftentimes used in some forms of wavelet analysis.

For the above reasons, a conception was creatively evolved by the undersigned in terms of a nonlinear-acoustic system that was capable of producing an ultrawide-band "impulse" in the shape of a quasi-Ricker wavelet for marine seismic exploration. In

using a far-field interacting SD/NLS system with a uniquely (what, later, was named Gauss-Rees) shaped Primary Waveform, highly repeatable Secondary Wavelets could be nonlinearly generated with shapes in the form of the desirable quasi-Ricker wavelet. Its "clean" unimodal spectrum was intended to be compatible with Predictive Deconvolution and facilitate "clear" data "stacking" capable of identifying "bright spots" and consistent with thin-layer Amplitude Analysis. It also was intended to provide an Energy Source Level (ESL) comparable to other high-energy sources enhanced by a directionality capability lacking in other sources. Consideration of the application of this highly attractive technology for land as well as marine seismic exploration came much later.

The advent of Ultra Wide Band (UWB) radar gave the conception of the nonlinear-acoustic, ultrawide-band sounding source technique and its related imaging technology an even greater boost. The limitations of the frequency dependent "skin effect" on enclosure penetration, it seemed, could be overcome by employing a "range-resolution" sonic equivalent of UWB radar because of the far less enclosure attenuation that would be encountered in the requisite sonic band. In this context, it is to be recognized that "range resolution" is given by $c_0/2W$, where c_0 is the propagation velocity in the medium under consideration, and W is the overall bandwidth in hertz located around a center frequency approximately equal to W/2 for an ultrawide-band wavelet.

Further, it is to be noted that an approximately 10^6 difference between 3×10^8 meters/second as the ElectroMagnetic (EM) energy-propagation speed and around 340 meters/second as the speed-of-sound at sea level in air. Whereas, the speed-of-sound underwater increases by a factor of roughly 5 to about 1,500 meters/second. Therefore, this 0.88×10^6 difference in propagation speeds between in-air EM radar propagation and in-air sound propagation also impresses the same scaling on the bandwidth, W, and the approximate center frequency of a roughly 100 % bandwidth-ratio wavelet if it is to retain equivalent "range-resolution" capabilities. For example, UWB radar centered, say, at $W/2 \approx 5$ GHz would have 0.015 meters (i.e., 0.59 inches) "range-resolution", with a sonic equivalent that could be center around $W/2 \approx 5$ .67 KHz for an in-water sonic system or $W/2 \approx 25$ KHz underwater.

It will be shown in the Summary of the Invention how the quasi-Ricker wavelet can be easily scaled to fit most "range-resolution" requirements. This requires careful choice of the Primary Wave frequency and Gauss-Rees waveform scaling in order to maintain a "down-shift" ratio around the favored 5:1 value that leads to acceptable conversion efficiency. Higher values degrade the conversion efficiency. However, when dealing with ultrawide-band Secondary Wavelets, care must be exercised by avoiding too low a value that can cause spectral overlapping between lower-band components of the Primary Waveform and upper-band components of the Secondary Wavelet.

All of these highly desirable wavelet repeatability, directionality and ultrawide-band imaging capabilities, plus the potential for material discrimination through applying spectroscopic analysis have motivated the generic invention described herein as being a Parametric Ultrawide Band Sounder (PUBS™). As such, PUBS™ is intended to serve as the basis of a Use Patent out of which various other Application Patents will evolve. It is

asserted that ownership of the generic PUBS™ techniques and associated technology will carry over to any application. However, this in no way precludes assignment to any individual or corporate entity under agreed terms covering the use of PUBS™ techniques or technology for a particular Application. As previously stated, it is maintained that these agreed terms will also include the assignee assuming the costs of any U.S or foreign Application Patent coverage and the subsequent costs to reduce-to-practice.

Summary of the Invention:

Based upon the analytic forms for near-field and far-field interaction expressed in the two formulations presented in the section on the Theoretical Precepts of the Invention, the complex Secondary Wavelet (when adjusted to represent that derived by SD/NLS system), respectively, is proportional to $\partial^2 |\varphi(\mathbf{x}, t')|^2/\partial t'^2$ and $\partial |\varphi(\mathbf{x}, t')|^2/\partial t'$. The undersigned first noted that, if $\varphi(\mathbf{x}, t')$ were a Primary Wave whose traveling wave form consisted of a Gaussian envelope modulating a Continuous Wave (CW) carrier, as given by the expression $\exp [-(a t')^2] \exp (-i \omega_0 t')$, then the Secondary Wave resulting from near-field interaction would be proportional to an inverted Mexican-hat wavelet, F(t'), which has the form $F(t) = -(2a)^2 [1 - (2at)^2] \exp [-(2at)^2/2]$. In other words, provided near-field interaction applies, a Gaussian shaped envelope modulating a CW carrier would provide a Secondary Wavelet having the desired quasi-Ricker wavelet form. Independently, both Berktay at Birmingham University in the U.K and Muir at the Applied Research Laboratory of the University of Texas discovered this relatively simple technique for generating such a wavelet.

However, the undersigned immediately recognized the limitations of this technique when the desire was to apply it to a wide range of system applications while expanding the range of this technology. This was particularly so if the desire were to apply it to marine seismic exploration requiring quasi-Ricker wavelets centered at, say, 54 Hz or wide azimuth sector, vertically directional ocean-basin surveillance sonar operating at around 150 to 300 Hz. In each case, the need for low operating frequencies, respectively, to achieve sea-floor penetration or long surveillance ranges, while using modest-sized arrays of electro-acoustic transducers, was by no means consistent with near-field interaction. Instead, the use of SD/NLS systems utilizing far-field interaction was indicated. The problem became one of how could the desired quasi-Ricker wavelet be generated when far-field interaction applied?

There are some who erroneously thought (and, perhaps still do) that the unique Gauss-Rees Primary Waveform, that was conceived to form the desired quasi-Ricker Secondary Wavelet, arose from a 30 year or more old Controlled Impulse Generator (CIG) technique. This CIG technique has long since been lost-in-the-sands-of-time; and, most likely, was never reduced-to-practice. The CIG technique also was conceived with conventional sonar rather than nonlinear acoustic (or parametric sonar) applications in mind. Namely, it basically was a linear transfer-function correction technique.

Unfortunately, directly applying the CIG technique to make up for the missing temporal partial derivative in the far-field interaction expression would require a

corrective frequency response of the form $|i(\omega - \omega_0)|$ applied around the carrier angular frequency, ω_0. Using this CIG-like corrective frequency response would suppress the carrier situated at an angular frequency $\omega = \omega_0$; thereby leading to the greater than 100 % type of **super modulation** originated by Taylor, who was an Amateur Radio operator in the U.K many eons ago. Even though it achieved vast communications distances using under the 100 watts of power mandated by the General Post Office, Telecommunications Branch in the U.K, such **super modulation** was banned. (At that time, the GPO was the U.K communications operating authorities governing Amateur Radio licensing.)

This was done because it introduced severe "side-band" energy "splash" and unduly distorted the speech communications waveforms. In a like manner, a CIG-like derived Primary Waveform would introduce similar unwanted spectral components with a consequential distortion of the sought-after quasi-Ricker wavelet. The ***uniqueness*** of the Gauss-Rees Primary Waveform results from reintroducing the correct amount of carrier to restore 100 % Amplitude Modulation (AM) and no more.

The form of the Gauss-Rees Primary Waveform – which, *in toto*, includes the product of a non-gated Gauss-Rees function and a gating function – that achieves this has a traveling wave form consisting of an envelope and carrier given by the multiplicative formulation $g(t') \{1 - (2at') \exp \{[1 - (2at')^2]/2\}\}^{1/2} \exp (i \omega_0 t')$. There are some insignificantly weak components arising from the temporal partial differentiation of the multiplicative action between the gating function, $g(t')$, and the non-gated form of the Gauss-Rees waveform. However, the temporal partial derivative – that is brought about by far-field interaction in the medium and, consequently, is applied to the square of the modulus of this complex Gauss-Rees waveform –results in a dominant waveform component which is proportional to the combined terms $F(t) [g^2(t) \exp (1/2)] / (2a)$. Wherein, F(t) is the desired inverted Mexican-hat wavelet. (This, of course, means that the Secondary Wavelet also has the sought-after quasi-Ricker wavelet properties.)

In this formulation, $g(t')$ is a suitable gating function that provides the Secondary Wavelet with a limited region of "***compact support***" that renders the wavelet "energy bounded" rather than having a restored carrier that is far longer than needed. It also is not so short as to prematurely truncate the desired quasi-Ricker wavelet that arises as a Secondary Wavelet from the action of a far-field SD/NLS system using a Gauss-Rees Primary Waveform. It also has leading and trailing edge tapering that, ideally, should be adjusted to avoid any significant edge discontinuities arising from the temporal partial derivative provided by far-field interaction in the medium.

With each "picture being worth one-thousand words", the following graphics, supported by narrative, are offered so as to pictorially demonstrate the generic **P**arametric **U**ltrawide **B**and Sounder (PUBS™) invention:-

Figure 1a represents a conceptual Primary Wave (Gaussian) spectrum required for a **near-field** SD/NLS system to produce the Figure 1b spectrum of a Secondary Wavelet having the corresponding temporal form of a quasi-Ricker wavelet or, synonymously, that of an inverted Mexican-hat mother wavelet. For reasons previously stated, generally,

such a near-field interacting SD/NLS system is limited to quite high frequency, short range operation. As such, it has a very limited range of utility.

Figure 2a illustrates the temporal wavelet shape of a Ricker wavelet; which is plus and minus three-quarter of a cycle of an inverted cosine wave and, therefore, represents one-and-one-half cycles of a symmetrically inverted cosine wave. Figure 2a shows a temporal Gaussian envelope of the **near-field** interacting SD/NLS system. Figure 2c indicates the intermediate wavelet shape that would exist after the application of a single temporal partial differentiation of this Gaussian envelope. Figure 2d shows that a quasi-Ricker wavelet would arise after the application of a second temporal partial derivative is applied. Although the artists impressions of Figures 2a and 2d are not drawn to represent it, the temporal average of the Ricker wavelet shown in Figure 2a is not zero; whereas, as needed to avoid violating hydrostatic-pressure properties, the quasi-Ricker wavelet shown in Figure 2d does have a zero temporal average. The temporal smoothness of a quasi-Ricker wavelet is contrasted with a typical air-gun signature in Figure 2d. Figure 2e shows the gated version of a carrier-borne Gauss-Rees Primary Wave required in the production of the quasi-Ricker wavelet shown in Figure 2d when one of the two temporal partial derivatives is not present when a **far-field** interacting SD/NLS system is used. By visualizing a bipolar carrier being modulated by the Gaussian envelope shown in Figure 2b, this may be contrasted with the Figure 2e carrier-borne Gaussian Primary Wave needed when a **far-field** rather than a **near-field** interacting SD/NLS system is utilized.

Figure 3a shows the "touching" base-band (one-sided) energy spectrum of a Ricker wavelet; wherein, the spectral side lobes should be noted along with the presence of a DC component indicating a non-zero temporal average. Figure 3b shows the (one-sided) energy spectrum of the Gauss-Rees waveform needed for the formation of a quasi-Ricker wavelet through a far-field interacting SD/NLS system. The central spectral component shown in Figure 3b represents how **super modulation** is avoided through the restoration of a gated CW carrier. If the Controlled Impulse Generator (CIG) technique – primarily devised with conventional sonar waveform correction in mind rather than the far-field interacting SD/NLS system approach – were applied, the need for this gated CW carrier component would not be revealed and ***no clue*** would be provided to ***proceed***.

Without this additional "gated" CW-carrier component, the DC offset of the carrier-modulating envelope shown in Figure 2e would be removed. In this case, the central "waist" region that exactly "touches" zero – consistent with 100 % amplitude modulation – would crossover, respectively, into both opposite negative and positive directions. Such **super modulation** would produce a spurious carrier "burst" filling the desired "trough" region. The Gauss-Rees Primary Wave is intended to correct this type of **super modulation**; which, otherwise, causes untenable side-band "splash" and resulting unacceptable quasi-Ricker wavelet distortion in any far-field interacting SD/NLS system!

Figure 3c shows the smooth (one-sided) spectrum of a quasi-Ricker wavelet. This wavelet spectrum and its corresponding temporal wavelet are highly repeatable. To the contrary, an air-gun marine seismic energy source spectrum has undesirable "ripples' due to a secondary "bubble" pulse. This is shown for contrast with the quasi-Ricker wavelet

energy spectrum both shown in Figure 3c. Although not shown, a multi-tip "sparker" marine-seismic energy source would exhibit an even more "ragged" energy spectrum. If the desire is to produce "clean" seismic, multi-channel data "stacking" or to employ spectroscopic analysis for discerning material-specific additional spectral components (that are induced by nonlinear interaction within or inelastic scattering from concealed material), a "clean" Secondary Wavelet energy spectrum is essential.

Figure 4a shows an un-gated Gauss-Rees Primary Waveform. A smoothly tapered version of a trapezoidal "gating" function is shown in Figure 4b. The multiplicative composite of these two functions is shown in Figure 4c. In this way, Figure 4c also is used to demonstrate that, without gating, there would be no discernible region of "compact support" to ensure bounded energy in the quasi-Ricker wavelet formed through far-field interacting SD/NLS system. Without gating, Primary-Wave energy would be wasted in regions outside of the intended Secondary Wavelet region of "compact support." The role of the DC offset should be noted in Figure 4c.

Figures 5a and b are used to illustrate a seismic energy-source case. Figure 5a shows the comparative temporally quantified Ricker and quasi-Ricker waveforms (respectively shown in dashed lines and in solid lines). A wavelet region of "compact support" 23 milli-seconds in duration is shown. As may be seen, the pair of zero crossings for the Ricker wavelet are closer together (i.e., 7.67 milli-seconds) than those for the quasi-Ricker wavelet set at 8.33 milli-seconds. The consequences of this become obvious from the (two-sided) energy spectral density characteristics shown in Figure 5b. These wavelets are both designed to have an energy spectral density that peaks at 54 Hz that is favored for deep seismic penetration of the Earth's hidden strata. Again, it is to be noted that the Ricker wavelet has a DC component – which could not be sustained by the hydrostatic-pressure encountered in marine seismic exploration – whereas, the quasi-Ricker wavelet has no DC component because it has a zero temporal average.

At this juncture, the artist's impressions are replaced with simulated Primary Waveforms and Secondary Wavelets. Figure 6 shows a side-by-side comparison of a "non-gated" Gauss-Rees Primary Waveform and the Secondary Wavelet formed by a far-field interacting SD/NLS system. The conversion efficiency indicated is about – 17.5 dB; which is about 6 dB more efficient than would be generated by an equivalent far-field interacting DW/NLS system otherwise using the same nonlinear parameters.

Figure 7a is the same temporal Secondary Wavelet as shown in Figure 6. This quasi-Ricker wavelet was simulated to arise from a "non-gated" Gauss-Rees Primary Waveform. Figure 7b shows the simulated (one-sided) energy spectrum of this quasi-Ricker wavelet. The a-parameter in the equation appropriate for this far-field interacting SD/NLS-system generated quasi-Ricker Secondary Wavelet was set consistent with the previously discussed 54 Hz marine-seismic energy source.

Figure 8 is similar to Figure 6 except a "first attempt" at designing a smoothed trapezoidal gating pulse has been demonstrated through simulation. As may be gleaned from this side-by-side temporal Primary Waveform/Secondary Wavelet comparison, the

gating pulse has too short a "flat top" and too rapid a rise and fall time to avoid pre- and post-Secondary-Wavelet "ripples"; even though this design would be highly energy efficient. Obviously "refinement" of this gating-pulse design is needed.

Nevertheless, Figure 9a repeats the same (somewhat distorted) temporal Secondary Wavelet as seen in the side-by-side Figure 8 comparison. This is done in order to show in Figure 9b the impact of the temporal Secondary-Wavelet distortion on the corresponding (one-sided) energy spectrum. Clearly the spectral "ripples" associated with this "first-cut" design of a gating pulse would impair any detailed spectroscopic analysis. A design "refinement" would be constrained to reduce these spectral "ripples" below a level acceptable to spectroscopic analysis.

Ducking this gating-pulse optimization problem at this phase of patent disclosure, attention is turned to scaling the Secondary Wavelet and its energy spectrum *via* altering the a-parameter. Figure 10 shows a Gauss-Rees Primary Waveform that has been scaled by 2:1 relative to its longer duration counterpart hitherto used for Primary Waveform to Secondary Wavelet demonstration purposes. In order to do this, the a-parameter has to be increased by 2:1.

Figure 11a shows the corresponding Secondary Wavelet generated by the Gauss-Rees Primary Waveform shown in Figure 10. It will be noted that, as anticipated, the resultant quasi-Ricker wavelet is shorter by a factor of 2:1. Figure 11b shows that the corresponding (one-sided) energy spectrum "stretches" by 2:1 and its peak moves up from the previous 54 Hz to 108 Hz.

This concludes a demonstration of the Primary Waveform/Secondary Wavelet characteristics and properties of the Gauss-Rees waveform and the quasi-Ricker wavelet generated by a far-field interacting SD/NLS system. The emphasis of these simulations has been to highlight efficiency as it relates to penetration and resolution as it applies to imaging. These aspects of the PUBS™ system techniques and related technologies, out perform UWB radar in terms of penetration and equals it in terms of resolution for imaging purposes.

However, the prospects for obtaining material properties *via* spectroscopic analysis of the impact of nonlinear material properties and hysteresis, as well as inelastic scattering, promises to significantly better UWB radar for non-intrusive remote sensing of concealed materials. This raises the question about how unique are the B/A-parameter ratio signatures for various gases, liquids and solids. Figure 12 attempts to address this issue by plotting the B/A-parameter ratios. As may be seen, although this represents a limited sample of gases, liquids and solids, the potential for separating various concealed materials on the basis of their nonlinear-acoustic B/A-parameter ratio appears promising.

Generally speaking, little attention has been given towards determining the B/A-parameter ratio for powdered materials ground from various substances. Based upon a private conversation with Professor Beyer (of Brown University), who is a renowned expert in nonlinear acoustics and related matters, the undersigned devised a way to

determine a derived B′/A′-ratio. This was handled by assuming crystalline grains of a material with a given B/A-ratio packed with a "void factor", v, and interstitial pores that were filled with a fluid (which could be a gas or a liquid). An expression was derived for composite material B′/A′-ratio in terms of a summation indexed over N-independent crystal-lattice modes. It also involved the density, ρ_C, the second-order, $M_{2,n}$, and third-order, $M_{3,n}$, elastic constants for the n^{th} crystal-lattice mode of the crystalline granular material. In addition, it involved the density, ρ_F, as well as A and B parameters of the fill fluid material.

Lacking material parameters for any illicit materials of interest to compare with a material with closely similar properties, two quite similar, relatively common materials were chose in order to separately apply the derived formula in order to make a B′/A′-parameter ratio comparison between them. The first material was Sodium Chloride (Halite) NaCl, which is a cubic crystalline-lattice material that is white, orange or red colored granulated or nodular material. The second material was Potassium Chloride (Sylvite) KCl, which also is a cubic crystalline-lattice material that is white, somet, grayish, bluish, yellowish or red colored granulated or nodular material.

Table-I provides a tabulation of the appropriate parameters for use in this formulation. In the case of these two different alkali halides, the b-parameter refers to the material hardness. It will be noted that, for these cubic crystalline-lattice materials, the summation index n = 1, 2, 3 will correspond to each of the three [100], [110] and [111] modes shown in the Table-I matrix for each of the two materials. In Table-I, derived elastic constants are set such that $M_{2,n} = K_{2,n}$ and $M_{3,n} = K_{3,n} + 3\ K_{2,n}$ in accord with a Thurston and Shapiro extension of the Breazeale and Ford treatment for cubic lattices.

Interstitial pores were assumed to be filled with air having A and B parameter values $A = 1.42 \times 10^5$ newtons/m and $B = 0.57 \times 10^5$ newtons/m, so that B/A = 0.4014. Random orientation of granules was assumed with a typical ± 5 % uniformity of granule sizes and a 40 %-porosity (i.e., the ratio of the volume of interstices to volume of mass) also was assumed. Using these parameters, the formulation yields $(B'/A')_{NaCl} = 6.0704$ and $(B'/A')_{KCl} = 4.8880$. These ratios are only minutely affected by variations in porosity (as is likely even when grain × fluid, *etc.* + higher-order terms are included), so that the 40 % porosity is hardly affected by the ± 5 % variation in grain sizes. For this reason, a ± 5 % coefficient-of-variation is assumed for the Gaussian statistical variation around the B/A-parameter ratio of each of the two composite materials.

The overlapping Probability Density Functions (PDFs) for each composite material both are shown on the ordinate axis of a graph plotted against a common B/A-parameter ratio, random-variate abscissa axis in Figure 13. A threshold equal to T = 5.4165 was set to provide a **symmetrical confusion matrix** which is shown in Table-II. This Table-II indicates that the two closely similar powdered materials chosen for this example may be separated correctly on the basis of their composite B/A-parameter ratios better than 98.4 % of the time and one mistaken for the other less than 1.6 % of the time. This is believed to be close to a ***worst-case*** situation in that, generally speaking, illicit

materials and the materials that should be found within a particular container would have more saliently different properties than the two materials used in the previous example.

The previous example considers separating pairs of inorganic materials. Some of the dangerous illicit materials of concern are organic in nature and, possibly, consist of living organisms. Tables III, IV, V and VI shown for various amino-acid groups demonstrate that the B/A-parameter ratio is significantly sensitive to small molecular changes. In each case, the mean and standard deviation of the B/A-parameter ratio is given. Armed with this information, by assuming a Gaussian PDF for each class, it would be entirely possible to construct a **confusion matrix** spanning all of these amino-acid classes.

The PUBS™ non-intrusive, remote sensor would assemble B/A-parameter ratio information through the application of spectroscopic analysis. Full separation of classes could be attempted on the basis of assembling a large classification **confusion matrix**. As a more practical alternative, PUBS™ could monitor the presence of specific illicit materials by passing over any test that did not reveal the presence of a material having one of these signatures. In this way, the test would essentially state that there is a very high likelihood that the illicit material or materials of concern is not present even though what is present is not identified. Any indication to the contrary would initiate a finer-grain search for illicit materials.

Another nonlinear-acoustic interaction that also could be utilized in a similar way involves the exploitation of acoustic Raman molecular scattering which is analogous to optical Raman scattering. As previously stated, investigations by both French and Soviet researchers strongly indicate that this mechanism is exploitable. Then, in the context of PUBS™ non-intrusive remote sensing, nonlinear-acoustic "impulse" interrogation similar to that performed by Nuclear Magnetic Resonance (MRI) spectroscopic imaging could be performed. The French research performed on a SASER also supports that acoustic energy transfer between states of molecular vibration does occur. Of course, phonon quanta, hv, values are far below photon-quanta values but a given acoustic power source creates a far higher phonon rate than the photon rate of its optical counterpart.

As with optical Raman (i.e., inelastic) scattering, acoustic Raman molecular scattering is expected to create (frequency down-shifted) Stokesian lines at frequencies not present in the original interrogation signal spectrum. This is due to energy being absorbed into an energy-state change caused by inelastic scattering. Likewise, (frequency up-shifted) anti-Stokesian lines also would appear. This is due to energy being given-up by an energy-state change caused by inelastic scattering collisions exciting the molecules in the material. These lines would appear around the non-frequency-shifted Rayleigh or Mie elastic scattering from molecules in the material under interrogation.

Analogous to optical Raman scattering, where Stokesian and anti-Stokesian lines, typically, are of the order of, respectively, 30 dB to 40 dB below Rayleigh or Mie scattered contributions, acoustical Raman molecular scattering might be considered as

having similar comparative levels for its Stokesian and anti-Stokesian lines. Again through analogy with optical Raman scattering, such acoustical emissions from inelastic phonon collisions are likely to be subjected to isotropic scattering. Therefore, these Raman scattered phonon emissions might be expected to be weak relative to the elastically scattered contributions from the far-field interacting SD/NLS system; wherein, these stronger components are utilized for B/A-parameter ratio statistical testing. Even so, because the Stokesian and anti-Stokesian lines have sharp "resonances" they will be quite discernible from the smooth quasi-Ricker Secondary Wavelet spectrum when subjected to narrow-band spectroscopy. Likewise, the signal-processing gain provided by spectroscopic analysis will effectively sizably increase the Signal-to-Noise Ratio (SNR) of the Stokesian and anti-Stokesian lines relative to the broadband noise associated with thermal agitation of the molecules within the material being interrogated.

Summary of Attributes of the Invention:

Consequently, it is asserted that **P**arametric **U**ltrawide **B**and **S**ounder (PUBS™) non-intrusive, remote sensing offers a better (and, perhaps, complementary) capability than Ultra Wide Band (UWB) radar. It does so by virtue of providing better enclosure-wall penetration while maintaining equivalent range and cross-range resolution for imaging purposes. In addition, its potential for providing concealed-material properties through nonlinear-acoustic interaction and hysteresis, as well as acoustic Raman molecular scattering from within the concealed material further exemplifies its use *in lieu* of or complementary to UWB radar.

Nothing Else Follows with the Exception of the Figures and Tables
Appearing on Page 20 of 32 Through Page 32 of 32 Inclusive.

FIGURE 1a: CARRIER BORNE ENERGY SPECTRUM

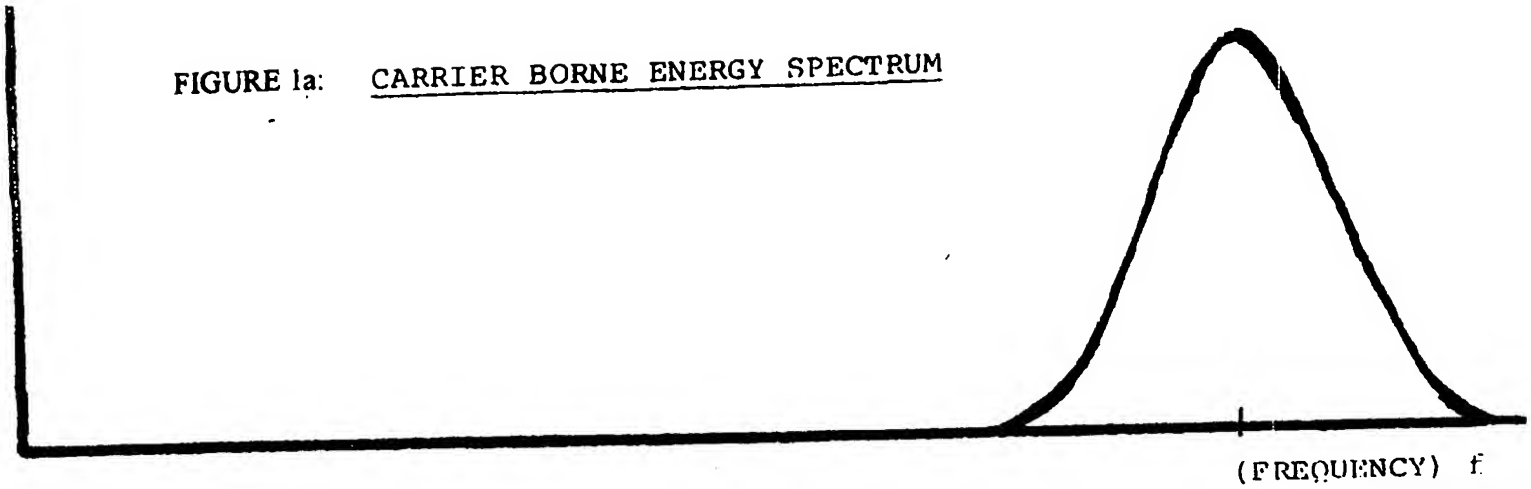

FIGURE 1b: SELF-DEMODULATED BASE-BAND ENERGY SPECTRUM

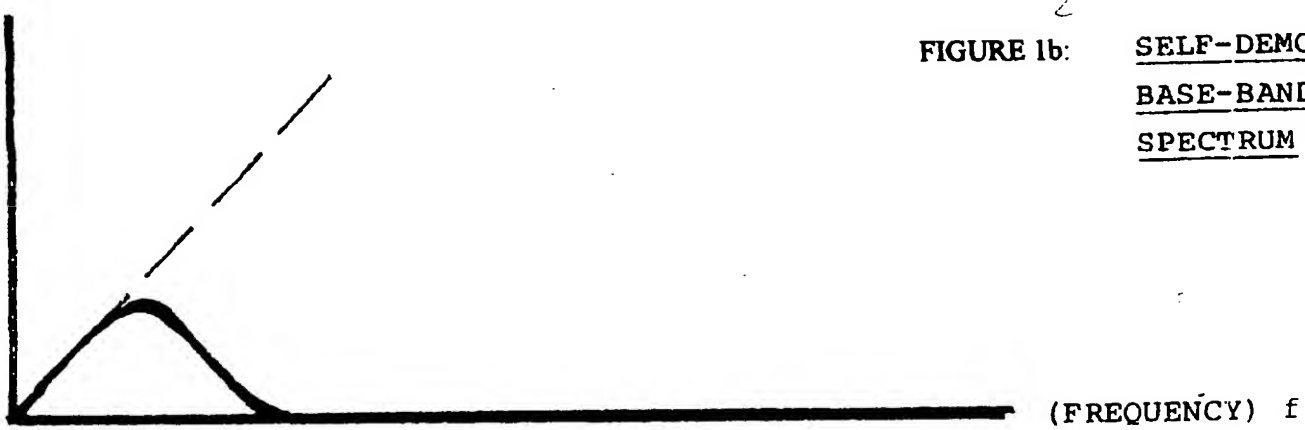

FIGURE 2a: RICKER WAVELET

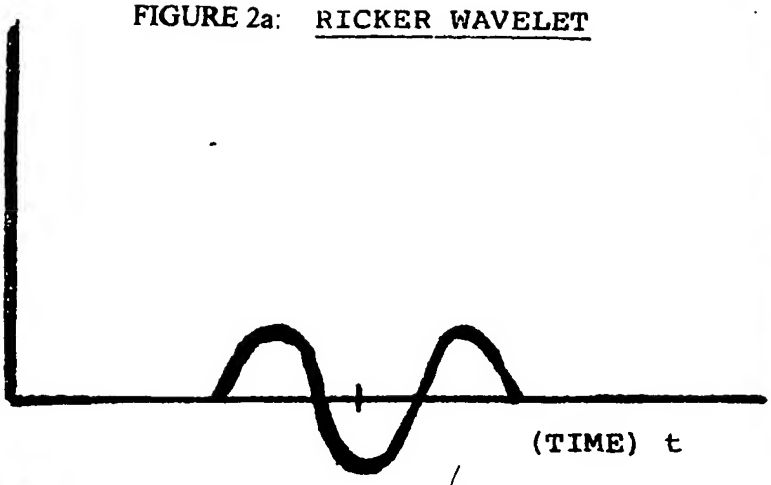

FIGURE 2b: GAUSSIAN WAVEFORM

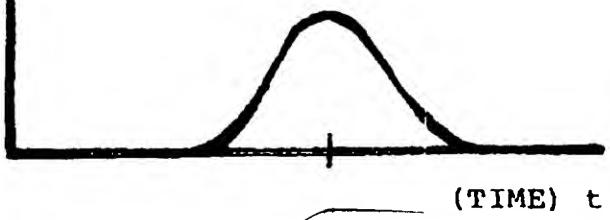

FIGURE 2d: SECOND DERIVATIVE OF GAUSSIAN WAVEFORM (QUASI-RICKER WAVELET) WITH AIR GUN SIGNATURE SUPERIMPOSED

FIGURE 2c: FIRST DERIVATIVE OF GAUSSIAN WAVEFORM

FIGURE 2e: PULSED CARRIER-BORNE WAVEFORM NEEDED TO GENERATE QUASI-RICKER WAVELET THROUGH NONLINEAR SELF-DEMODULATING, FAR-FIELD INTERACTION

FIGURE 3a: ENERGY SPECTRUM OF RICKER WAVELET

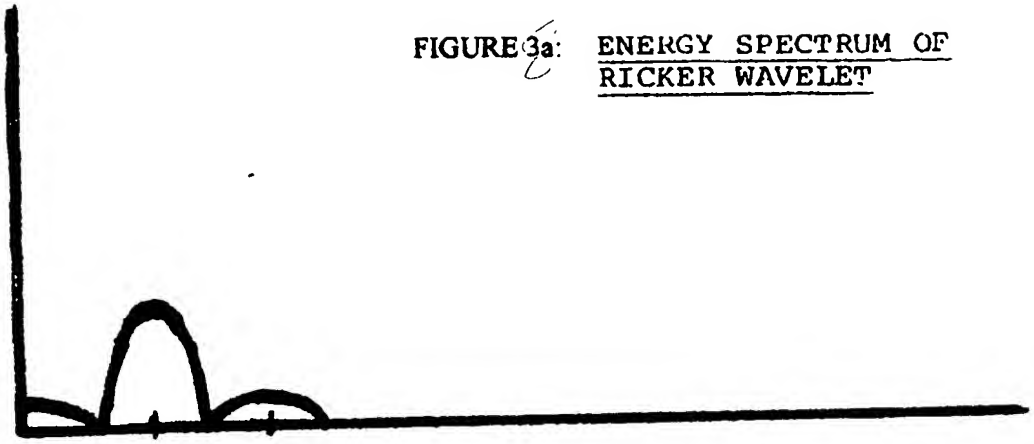

FIGURE 3b: ENERGY SPECTRUM OF CARRIER-BORNE WAVEFORM NEEDED TO GENERATE QUASI-RICKER WAVELET

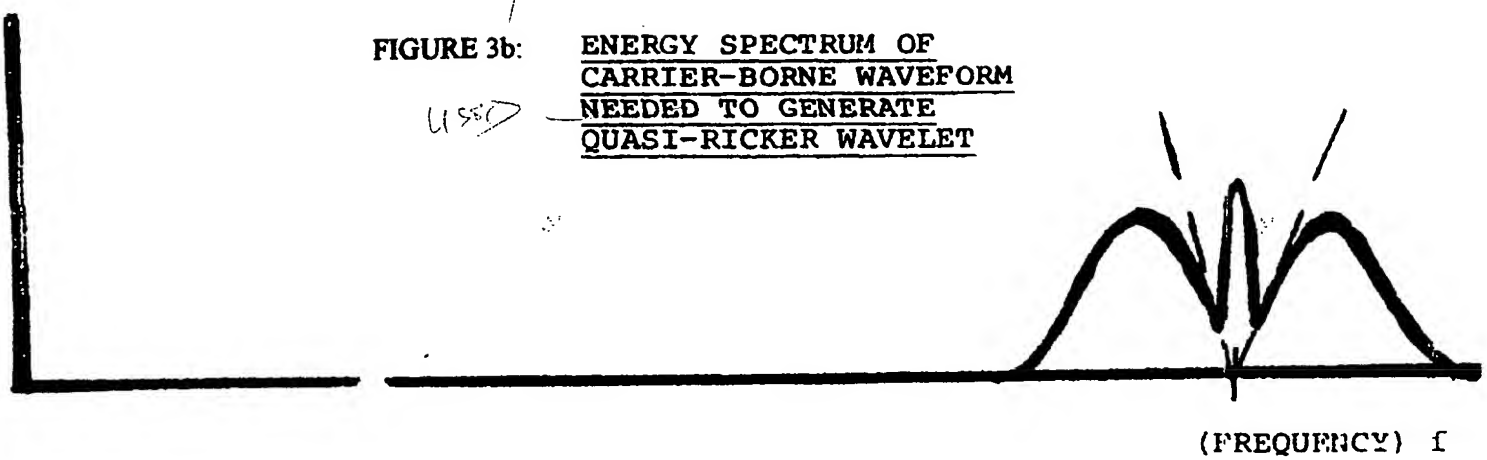

FIGURE 3c: ENERGY SPECTURM OF QUASI-RICKER WAVELET WITH AIR-GUN ENERGY SPECTRUM SUPERIMPOSED

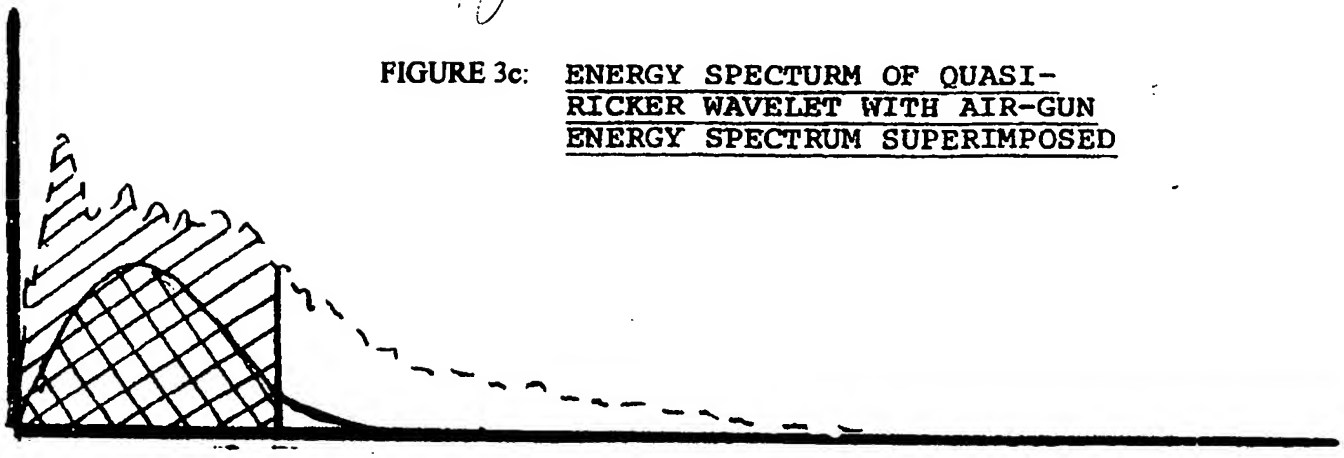

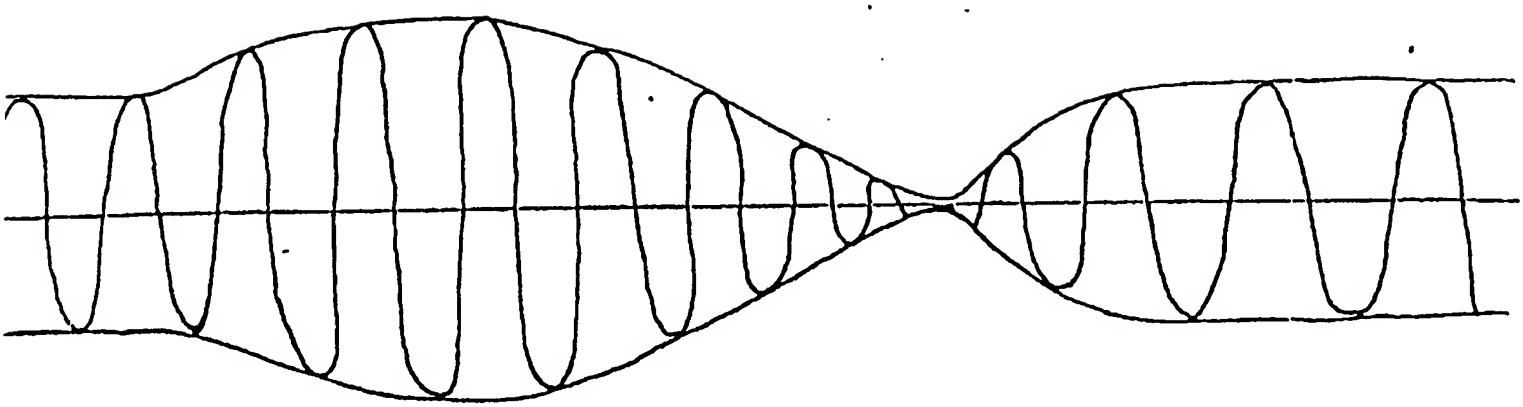

FIGURE 4a: PREDISTORTED (I.E., FIRST-DERIVATIVE) GAUSSIAN WAVEFORM PLUS DC OFFSET

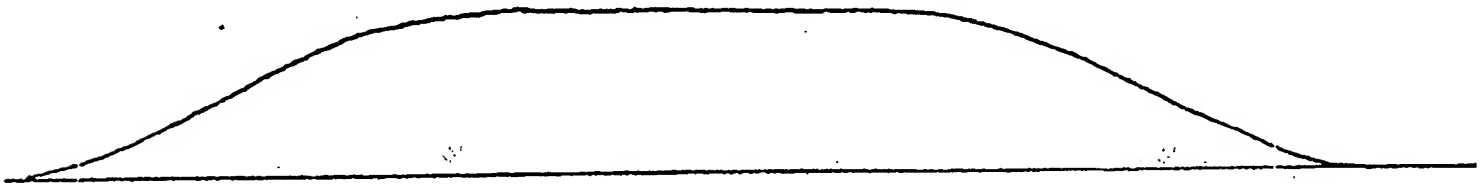

FIGURE 4b: TAPERED ENVELOPE GATING FUNCTION

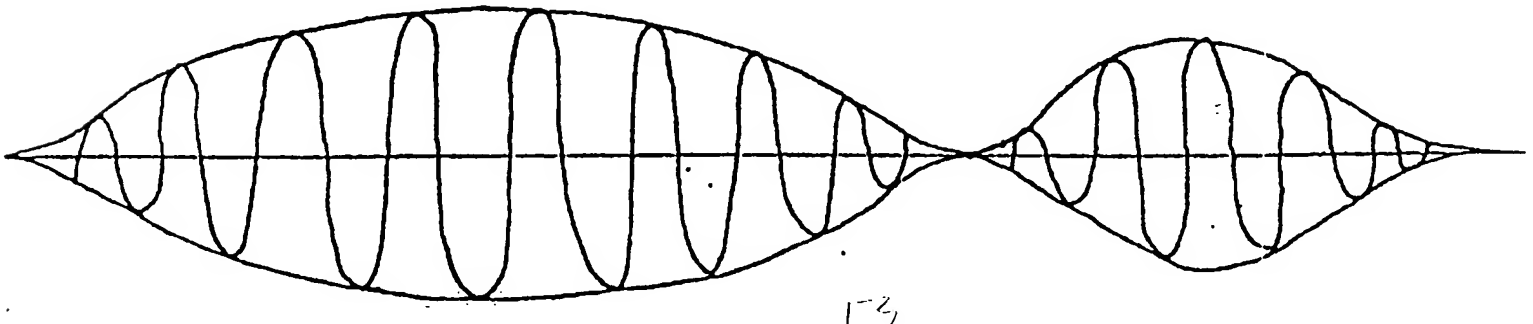

FIGURE 4c: COMPOSITE OF TAPERED GATING FUNCTION AND PREDISTORTED GAUSSIAN WAVEFORM

14

FIGURE 5a: TIME WAVEFORMS OF A QUASI-RICKER WAVELET AND A RICKER WAVELET

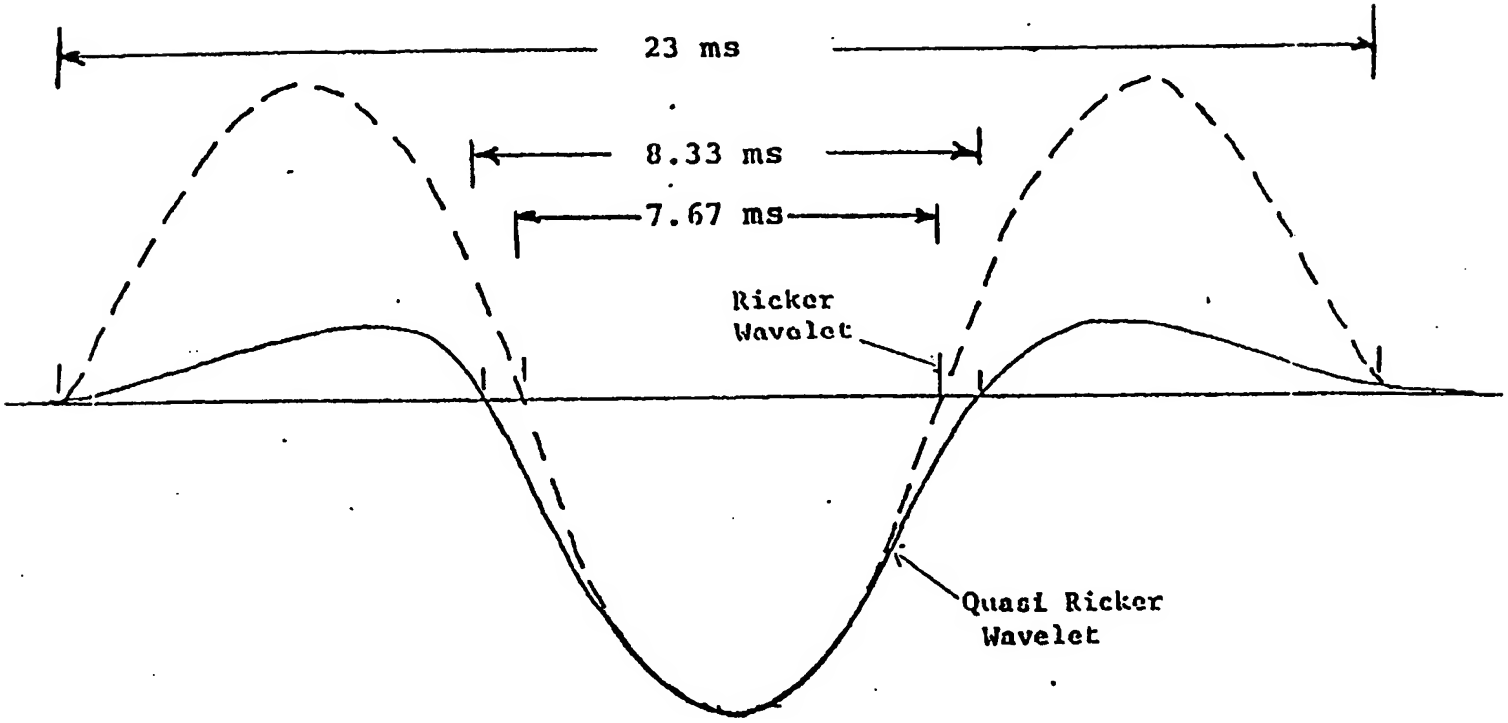

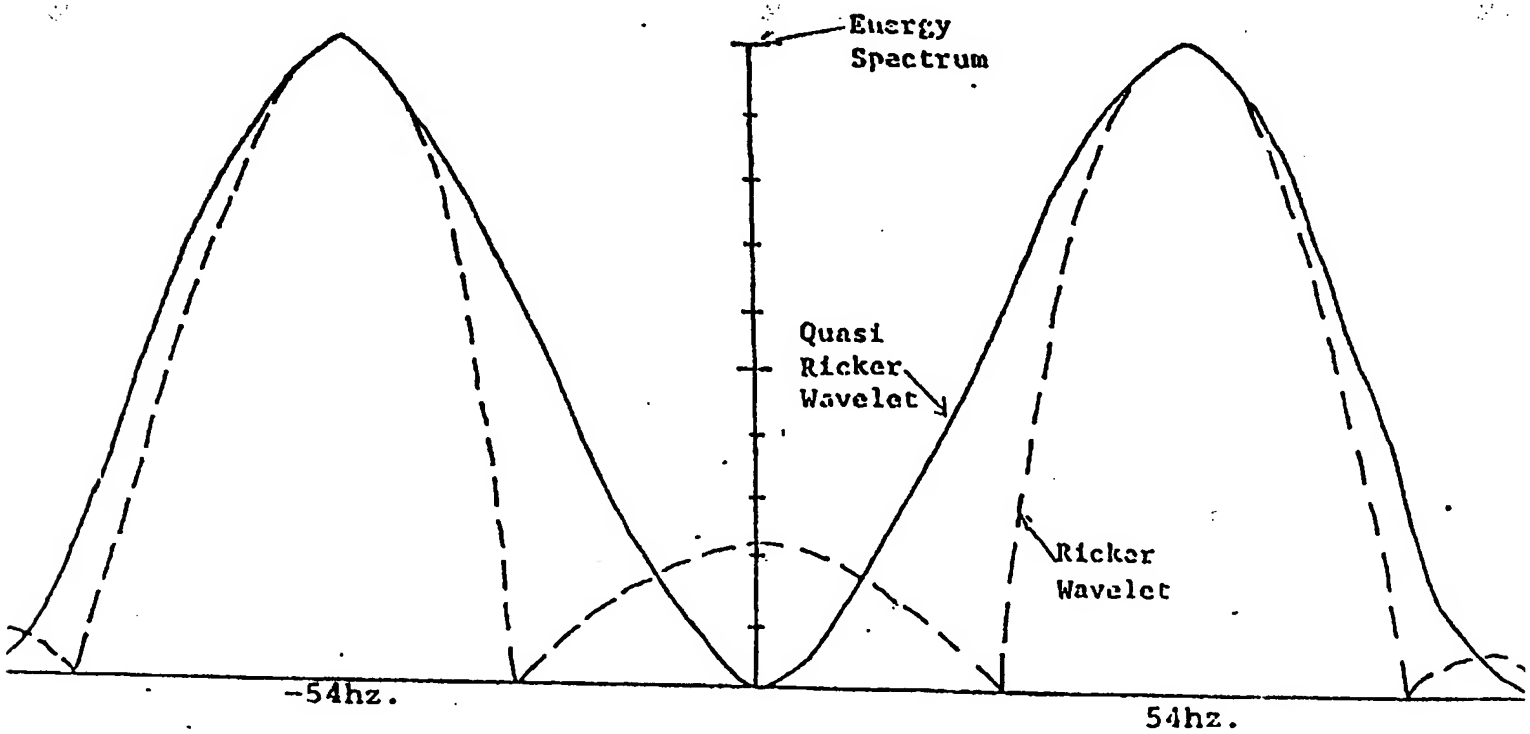

FIGURE 5b: ENERGY SPECTRUM OF A QUASI-RICKER AND A RICKER WAVELET

FIGURE 6: NON-LINEAR/PARAMETRIC SONAR

- Non-linear propagation characteristics of medium cause high frequency, high source level waveform to demodulate itself to a low frequency waveform.

- Demodulated waveform is proportional to first derivitive of transmitted waveform envelope.

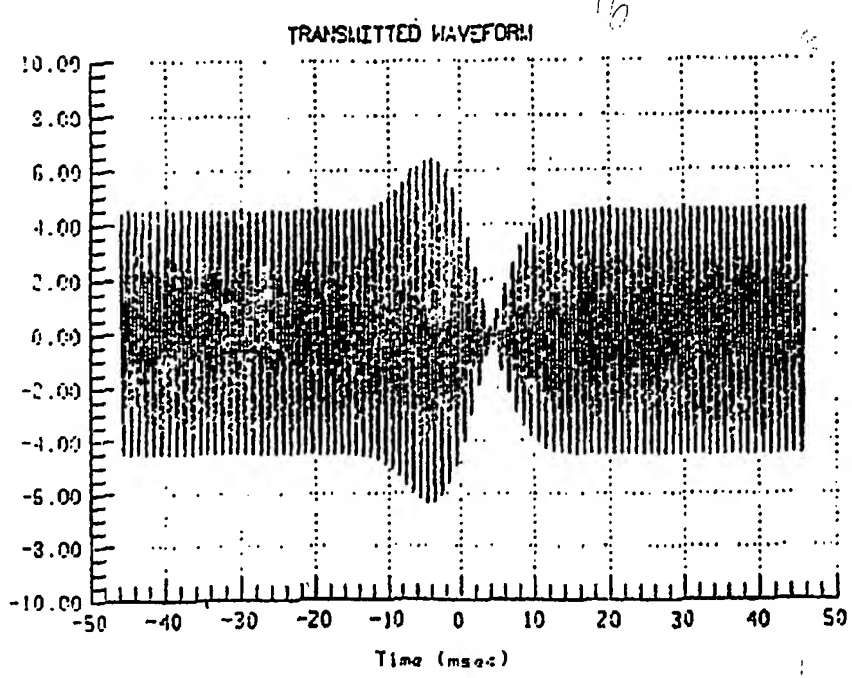

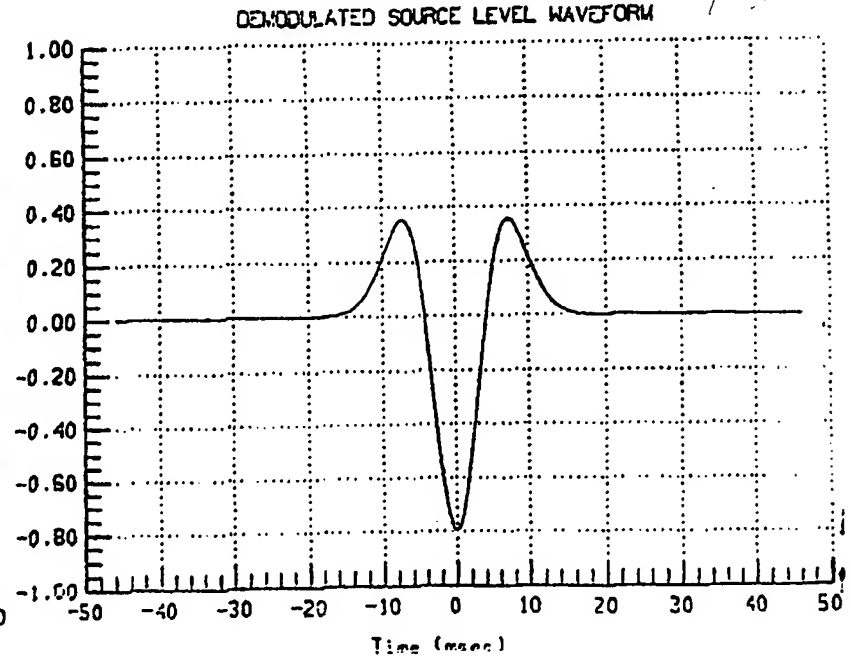

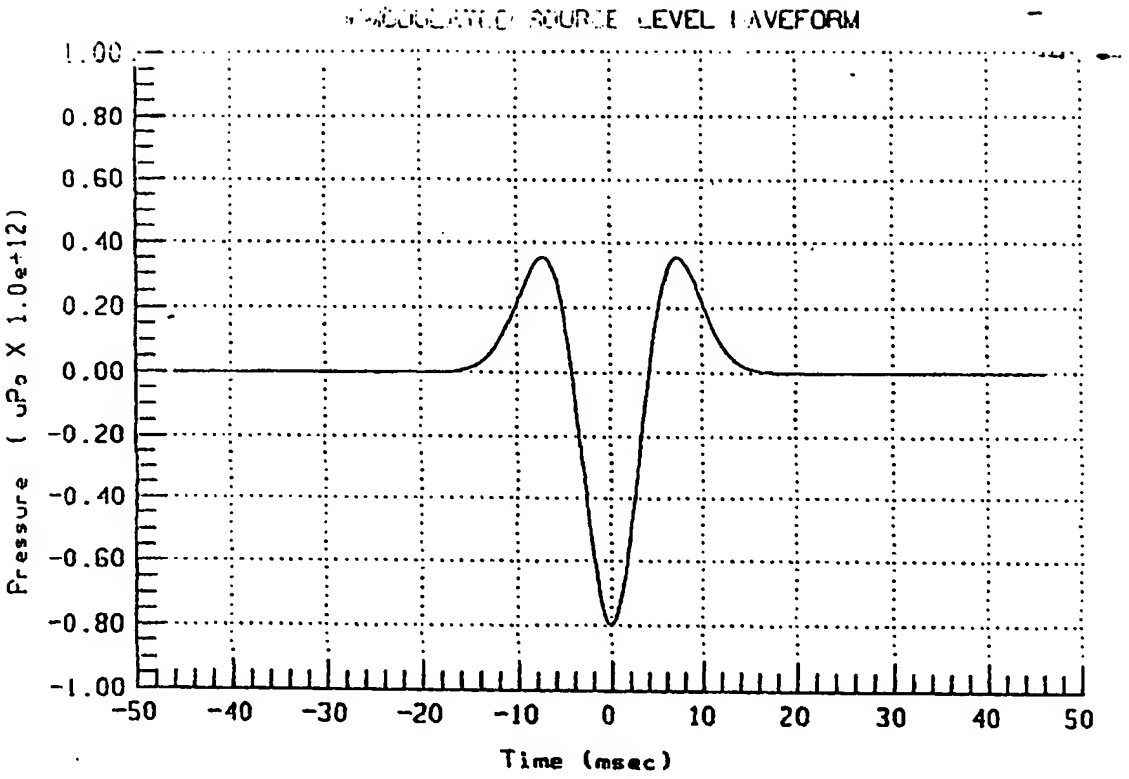

FIGURE 7a

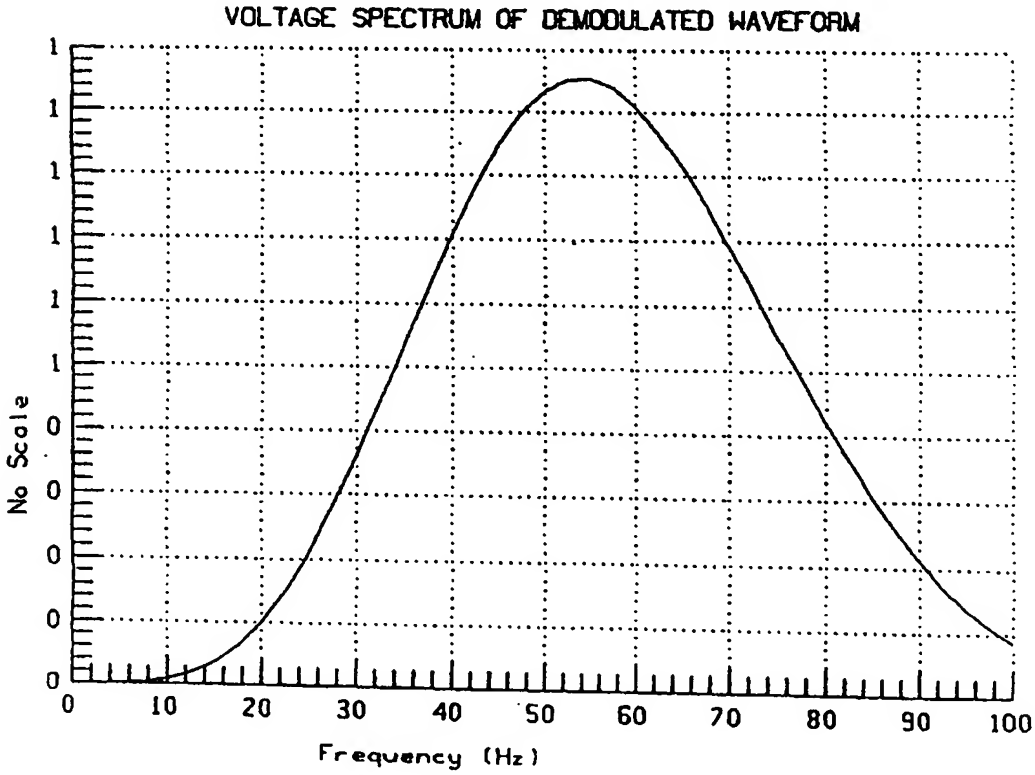

FIGURE 7b

FIGURE 8: PARAMETRIC SONAR WAVEFORMS

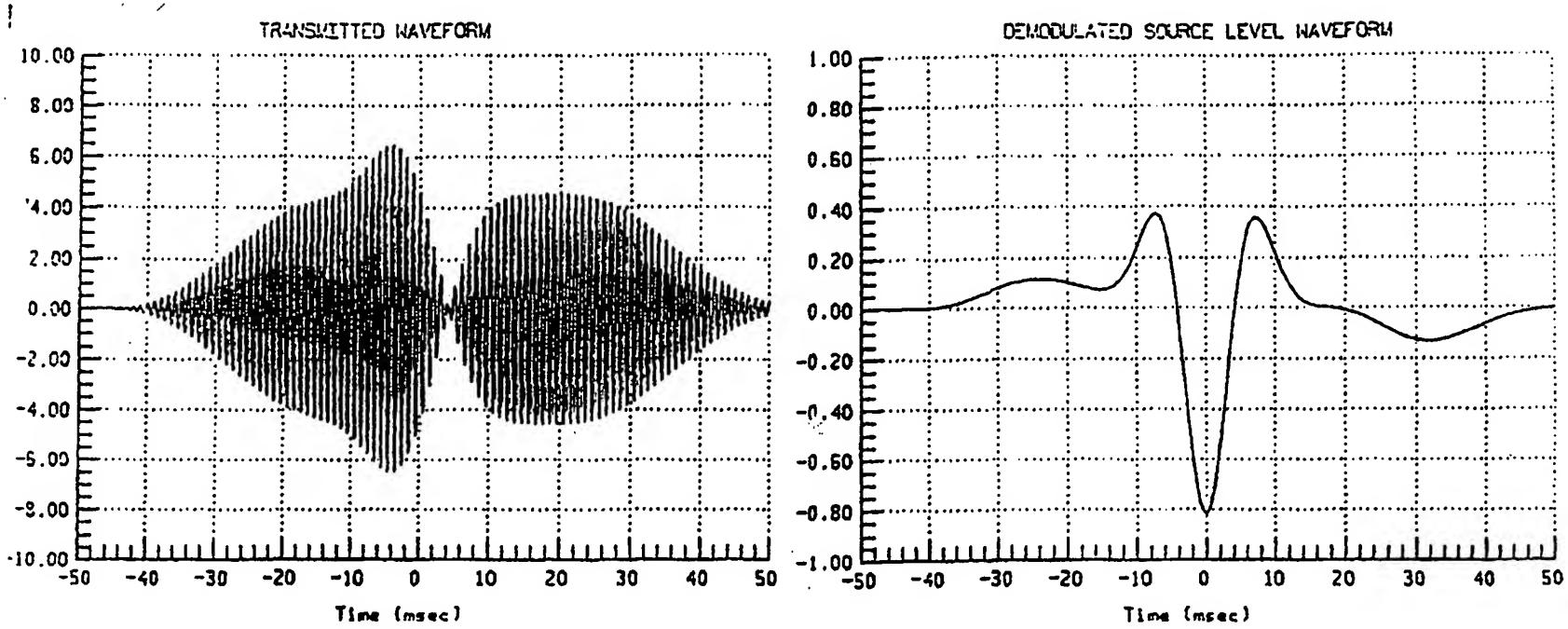

$$\varphi(\vec{r},t) = -D^2(\theta,\Phi)\,\frac{\beta R_0^2 P_0^2}{2\rho_0 c_0{}^3 r}\,\ln\left[\frac{\pi^2 f_s}{\alpha_T c_0}\right]\frac{\partial|\psi(t')|^2}{\partial t'}\,e^{(-\alpha_s r)}$$

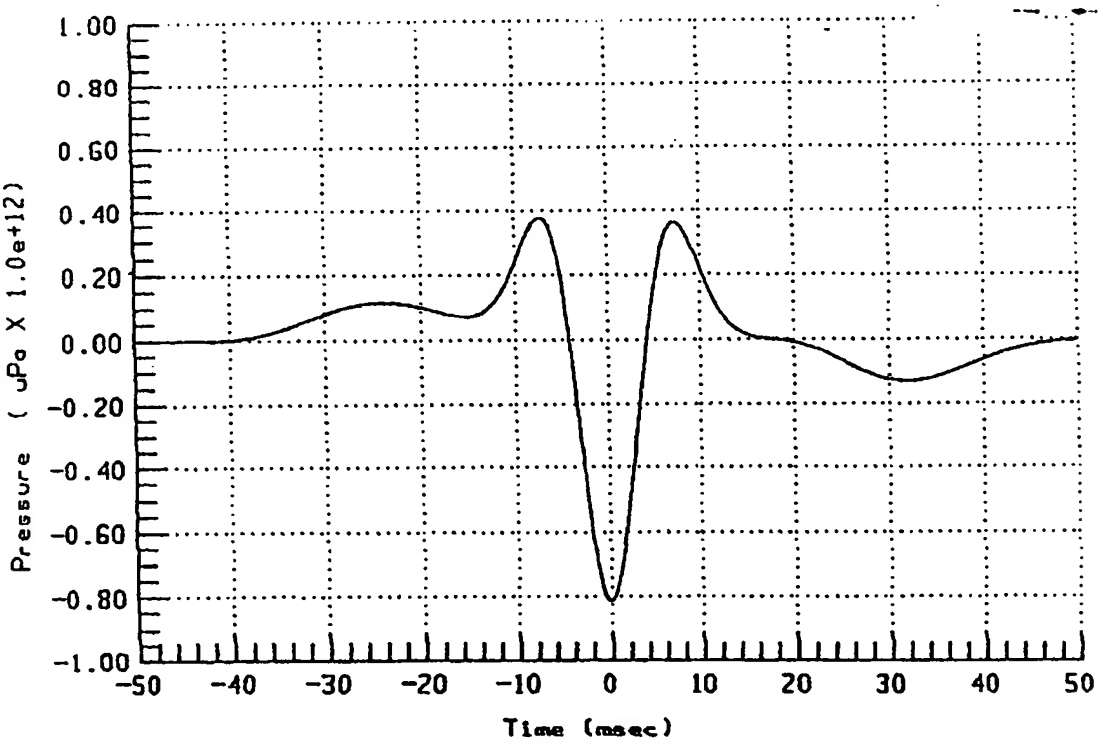

FIGURE 9a

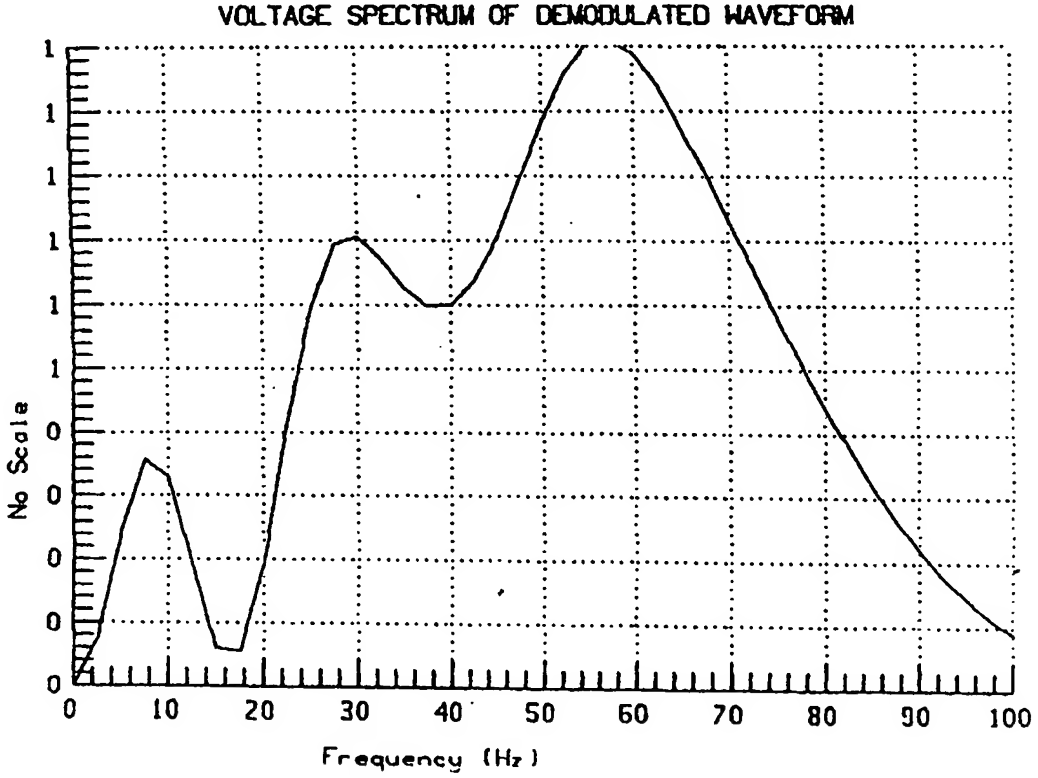

FIGURE 9b

TIME-SCALED TRANSMITTED WAVEFORM

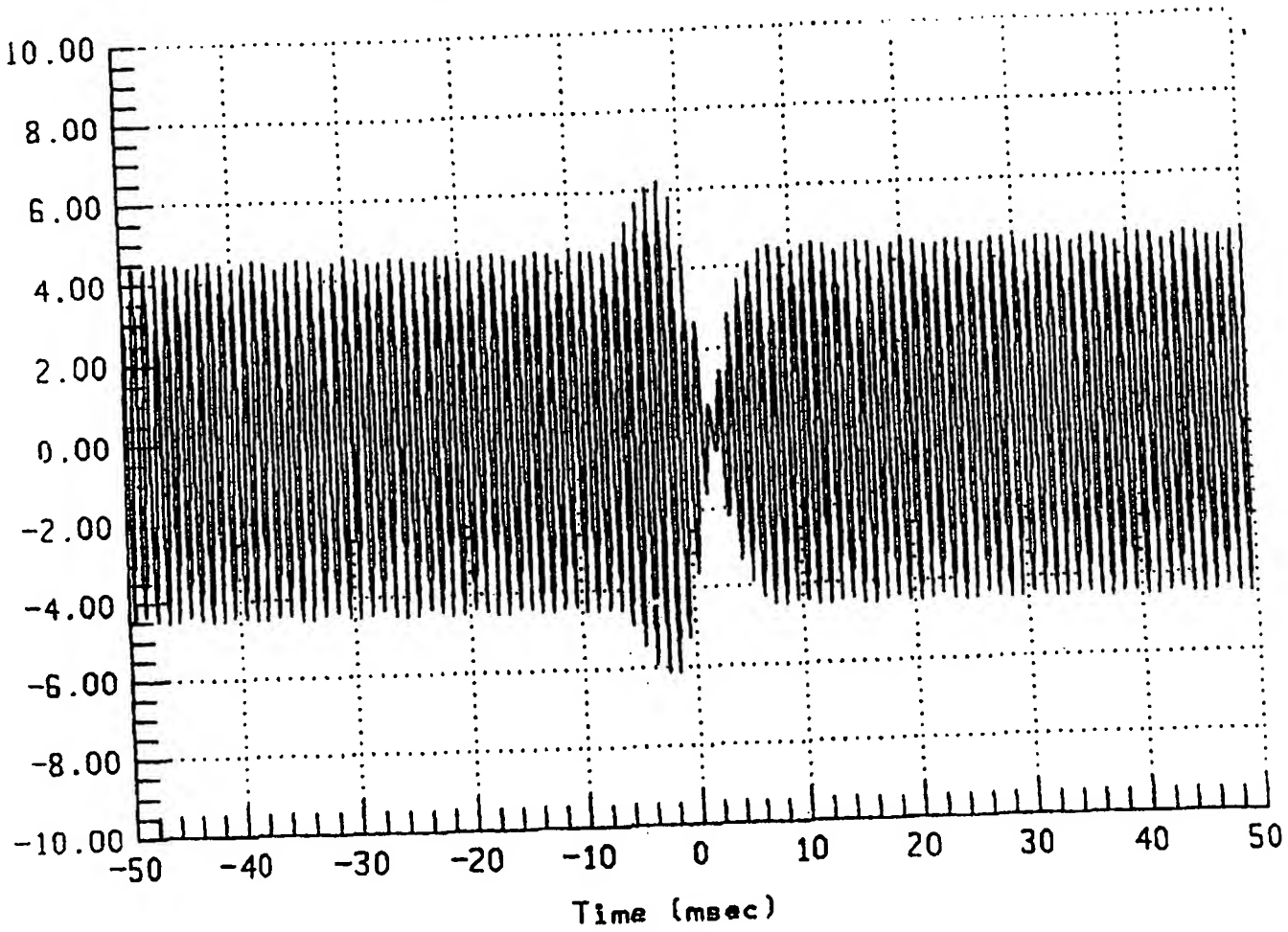

FIGURE 10

25

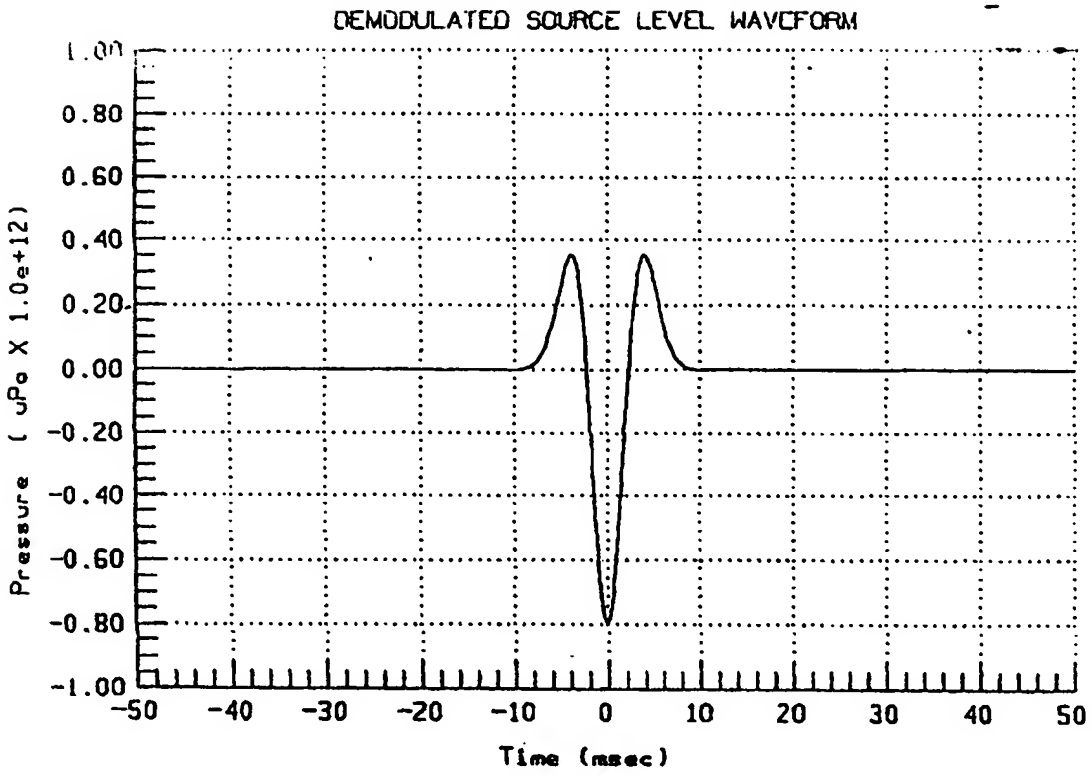

FIGURE 11a

26

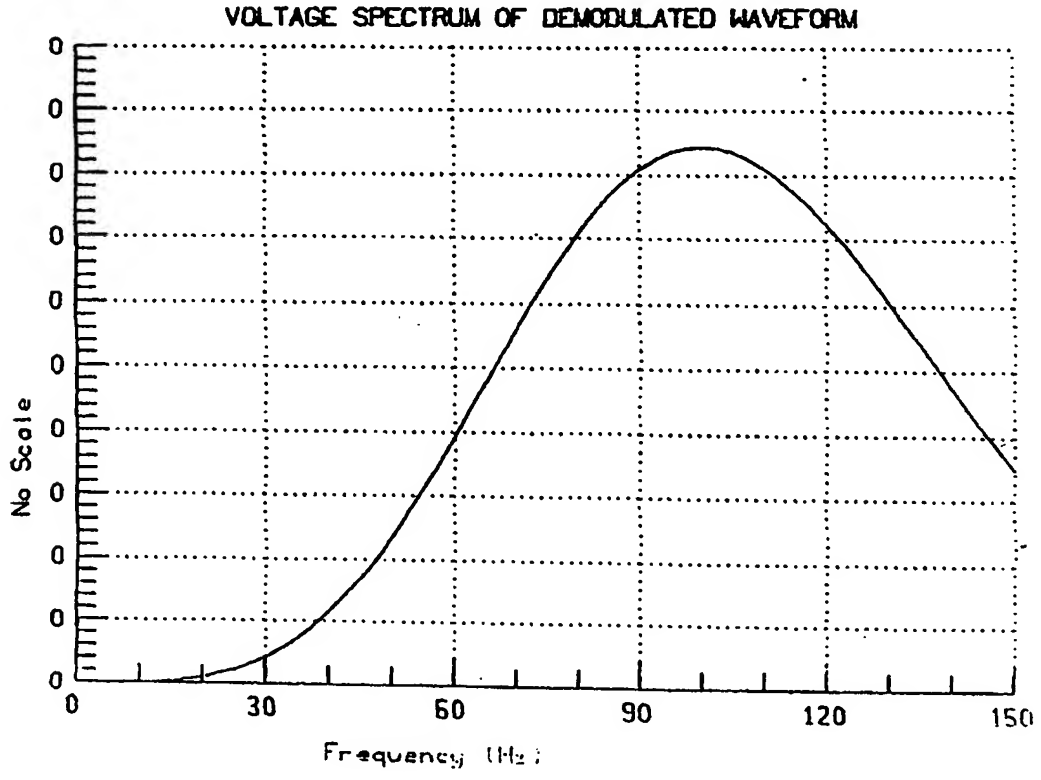

FIGURE 11b

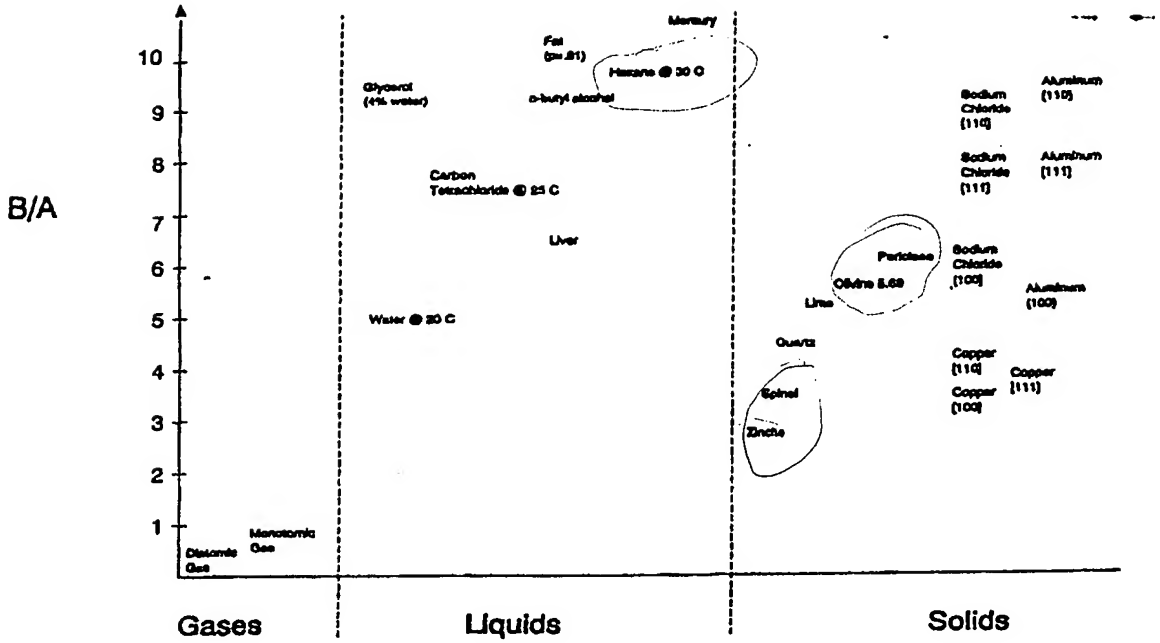

FIGURE 12: TYPICAL B/A-PARAMETER RATIOS FOR GASES, LIQUIDS AND SOLIDS

S. Crystal No.	Direc-tion	Longitudinal Velocity km/s	$\partial c/\partial p$ km s^{-1} $kbar^{-1}$	K_2 10^{+11} dyn/cm^2 (10^{+10} Newtons/m^2)	K_3 10^{+11} dyn/cm^2 (10^{+10} Newtons/m^2)	$-M_3/M_2$
Sodium chloride	[100]	4.767	0.046	4.98	-86.05	14.4
	[110]	4.485	0.029	4.38	-42.60	6.7
b = 0.288	[111]	4.403	0.019	4.20	-20.10	2.0
Potassium chloride	[100]	4.540	0.050	4.04	-60.13	12.0
	[110]	3.905	0.028	3.00	-22.42	4.5
b = 0.309	[111]	3.670	0.017	2.60	-12.12	1.7

TABLE I: ACOUSTIC NONLINEARITY PARAMETERS IN SOME CUBIC CRYSTALS NEAR 25 ° C

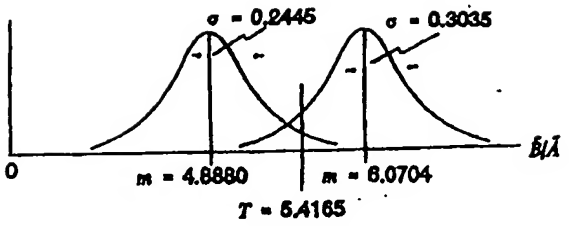

FIGURE 13: PROBABILITY DENSITY FUNCTIONS AND SYMMETRICAL SEPARATION THRESHOLD FOR THE B'/A'-PARAMETER RATIOS OF NaCl AND KCl COMPOSITE MATERIALS

		DECLARED	
		NaCl	KCl
TRUE	NaCl	0.984	0.016
	KCl	0.016	0.984

TABLE II: SYMMETRICAL CONFUSION MATRIX FOR THE STATISTICAL SEPARATION OF NaCl AND KCl ALKALI HALIDES BASED UPON COMPOSITE B'/A'-PARAMETER RATIOS

TABLE III. Sensitivity of the concentration increment of the nonlinearity parameter B/A to changes in the character of solute-solvent interactions and to the structure of the hydration shell.

AMINO ACID	GLY	ALA
Diagram of the hydration shell		
Physical nature of the solute-solvent interactions	Hydration shell is formed by electrostatic solute-solvent interactions. Dipoles of water molecules are attracted and oriented in the field of $-NH_3^+$ and COO^- atomic groups.	Hydrophobic $-CH_3$ group changes the structure of the hydration shell and limits accessibility of water molecules to the charged groups of the solute.
$\Delta(B/A)/C$ (cm^3/mol)	400 ± 20	270 ± 20

TABLE V. Sensitivity of $\Delta(B/A)/C$ of amino acids to structural isomerism in the side chains having the same amount of carbon atoms.

AMINO ACID	VAL	nVAL	GLN	PRO
Chemical structure		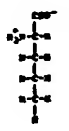	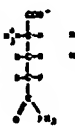	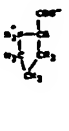
$\Delta(B/A)/C$ (cm^3/mol)	230 ± 20	170 ± 20	730 ± 40	190 ± 20

TABLE IV. Sensitivity of the nonlinearity parameter to the replacement of a single atomic group within a molecule. (Replaced group is shown by a dashed-circle.)

AMINO ACID	ALA	PHE	HIS
Chemical structure			
$\Delta(B/A)/C$ (cm^3/mol)	270 ± 20	400 ± 100	710 ± 70

TABLE VI. An example of striking sensitivity of $\Delta(B/A)/C$ to a change of the position of one atomic group within the same molecule.

AMINO ACID	LEU	ILE
Chemical structure	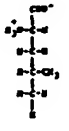	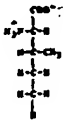
$\Delta(B/A)/C$ (cm^3/mol)	50 ± 20	180 ± 20

TABLE III, IV, V & VI: DISCRIMINATION OF AQUEOUS SOLUTIONS OF AMINO ACIDS BASED UPON THE ACOUSTIC NONLINEARITY B/A-PARAMETER RATIOS


OIPE
JUN 22 2006
PATENT & TRADEMARK OFFICE


OIPE
JC48
JAN 22 2002
PATENT & TRADEMARK OFFICE